Aalto University
School of Engineering
Department of Mechanical Engineering

Gregor Gruber

Development of a large scale bearing element thickness variation measurement device

Final Project
Espoo, March 21, 2016

Supervisors: Prof. D.Sc. (Tech.) Petri Kuosmanen (Aalto University)
Prof. Dr.-Ing. Stephan Rinderknecht (TU Darmstadt)
Advisors: D.Sc. (Tech.) Thomas Widmaier (Aalto University)
M.Sc. Lukas Quurck (TU Darmstadt)

Author
Gregor-Julian Benedikt Gruber

Title of thesis
Development of a large scale bearing element thickness variation measurement device

Major/minor
Industrial Engineering/Mechanical Engineering

Thesis supervisor
Prof. D.Sc. (Tech.) Petri Kuosmanen (Aalto University)
Prof. Dr.-Ing. Stephan Rinderknecht (TU Darmstadt)

Thesis advisor(s)
D.Sc. (Tech.) Thomas Widmaier (Aalto University)
M.Sc. Lukas Quurck (TU Darmstadt)

Date 21.03.2016 **Number of pages** XII + 52 **Language** English

This work describes the development and testing of a new type of bearing element thickness measurement device specifically designed for large scale bearings. The device is built around a sensor head featuring two tactile sensors that enable differential measurement of the thickness.

After analyzing an older prototype the new device and corresponding software that was developed as part of this work is explained in detail. Those chapters focus on the features that were built into the device to improve measurement quality and ease of use in general. Based on the design an actual machine prototype was built and tested against a reference grade coordinate measurement machine.

Through repeated comparative measurement and statistical analysis the measurement quality was assessed in terms of repeatability, trueness and other parameters. Examining the measurement results from both devices the feasibility of using such a device and its advantages and disadvantages compared to a conventional machine are discussed.

Keywords
Large Scale Bearing Elements, Bearing Element Thickness, Thickness Measurement, Differential Measurement, Differential Thickness Measurement, Measurement Machine Design, Rotating Measurement Machine, Rotating Bearing Measurement Machine, Moving Measurement Machine, Runout Measurement, Thickness Variation Measurement

Acknowledgement

I would like to take this opportunity to thank everybody that has contributed to this work and/or my academic career in general. This of course includes my friends who helped me get this far and who were also involved in finalizing this report.

The IMS Darmstadt, Prof. Stephan Rinderknecht and Lukas Quurck enabled me to go to Finland and broaden my horizon in many ways. I was fortunate enough to have already done my bachelor's thesis at this institute working on another project.

The people at MIKES and particularly Björn Hemming made it possible to get the reference measurements done quicker than expected and continued working even after I already had left Finland. I am grateful for the work you did and the time you spent contributing to this project.

I would like to thank everybody I met at the department of mechanical engineering at Aalto University. Prof. Kuosmanen made it possible for me to come there and helped me with a lot of things, like finding accommodation, which I would not usually have expected him to. Thank you for supporting me and my ideas but also for disagreeing and discussing them with me, both in the right amount. Thomas Widmaier was the first person in Finland I contacted before starting the project and without him I could not have managed to get it started so quickly. He and Jari Juhanko also supervised my work and guided me in the right direction. Ville Klar quickly became a good colleague and friend to me and I thoroughly enjoyed our weird and wonderful conversations. I would also like to thank Jouni Pekkarinen because without him realizing my design in this short time frame would not have been possible. Last but not least I would like to especially thank Raine Viitala for showing me the real Finland, advising me with my work and becoming a true friend. I am looking forward to seeing you all again someday.

As this thesis marks the preliminary conclusion of my academic career I thank my parents Edith and Ludwig Gruber for supporting me throughout all these years, believing in me and helping me to follow my dreams of becoming an engineer.

Index

List of figures

List of tables

List of abbreviations

Abbreviation	Meaning
CAD	Computer Aided Design
CMM	Coordinate Measurement Machine
FFT	Fast Fourier Transformation
JCGM	Joint Committee for Guides in Metrology
TMM	Thickness Measurement Machine
UPR	Undulations Per Rotation

1 Introduction

1.1 Background

Large scale bearings are one of the important elements of industrial machines. Especially in the field of power generation these bearings are used extensively. Renewable energy sources, where large scale bearings are used for example in wind turbines, have increased their share of the global energy market in the last couple of years (IEA 2015a, p. 4). This trend is projected to steadily continue in the coming years (IEA 2015b, p. 1).

In this area performance and reliability of the components is very important as downtime is not only costly but energy production is considered critical infrastructure. Applications such as off-shore wind parks pose new challenges in terms of bearing quality as the bearing sizes are very large and maintenance is difficult because of that as well as because of the accessibility of such locations. The logistics involved in repairing a wind power generator on the open sea bear a large economic risk and therefore play a role in the economic viability of this renewable energy source. As these applications become more common the issues are likely to become worse (EURAMET/EMRP 2015, p. 1). To ensure the production quality and operation of these bearing components and thereby mitigating the risk of failure metrological control is necessary.

> *"The protection of the environment from the short-term and long-term destructive effects of industrial activity can only be assured on the basis of accurate and reliable measurements"* (Placko 2006, p. 15).

One of the determinants of the quality of a bearing is the thickness deviation of the inner and outer rings. The reason for this is that these elements are comparatively thin in contrast to the housing and shaft they will be mounted to. This means the rings will conform to the shape of the adjacent parts in a way that their own roundness becomes less important. The thickness however is not affected by the mounting process in any significant way. Therefore this geometric variable of the bearings shape can influence the clearance within the assembled bearing and thus the rotational accuracy.

Measurements of the thickness can be taken with existing methods and devices such as coordinate measurement machines (CMM) and some specialized, two sided roundness measurement devices. These devices however are general purpose measurement machines and so their adaptability comes at the cost of less optimization for a single application. In an approach to help improve these thickness measurements and possibly widen the area in which they are used by way of constructing a specialized device the idea of this thesis was conceived.

1.2 Research Question

This thesis was focused around the following research question:

> Can a dedicated measurement device for ascertaining the thickness and thickness variation of large scale bearing elements be made in a way that it improves performance in terms of measurement quality, cost and/or ease of use when compared to existing devices in the same application?

This question was developed on the background laid out in the previous subchapter as well as based on work previously done at Aalto University. Here a prototype device for the same purpose was constructed as a proof of concept. This work is in part based on that prototype but emphasises evaluating the actual feasibility of using such a device as a replacement for conventional measurement machines. Doing so involves the following steps:

1. Analysing existing measurement devices and the previous prototype
2. Finding alternative concepts or improvements on existing concepts
3. Comparing these concepts and selecting a concept for further study
4. Making a design based on the chosen concept
5. Constructing a prototype device based on the design
6. Testing and evaluating the performance of the prototype
7. Giving recommendations on how to further improve thickness measurement

The structure of this thesis was devised to reflect these steps but also extend on them in regards to background information and basic metrology knowledge. Steps 1-2 are covered in chapter 2, steps 3-5 are described in chapter 3.1 as well as chapter 3.2 and finally steps 6 and 7 are a major part of chapters 3.3 to 5.

2 State of the art

In this chapter the state of the art as a basis for the concept and design of measurement devices in general and specifically the developed device will be laid out. To avoid ambiguity it is necessary to explicitly define some metrological terms. These will then be used in the explanation of measurement methods and existing devices as well as throughout this work.

2.1 Definitions

Measurand

The Joint Committee for Guides in Metrology defines measurand as:

> *"[A] particular quantity subject to measurement"* (JCGM 100:2008, p. 50).

In practice this means a measurable attribute of something that has been or is to be determined. An example of this relating to the topic of this thesis would be the thickness of a given bearing element. Technically the thickness is measured at many different points so each individual value could be interpreted as a separate measurand.

True value

> *"[The] value consistent with the definition of a given particular quantity"* (JCGM 100:2008, p. 32).

The true value is therefore the theoretical measurement result which would be obtained by perfect measurement. Because every measurement is by nature imperfect the true value cannot be determined by measuring. The objective of any measurement is therefore to determine a range in which the true value is to be found with a certain likelihood. Sometimes an exact number is given for a value, if this is the case it should be called "conventional true value" as it represents an assumption on the most probable true value (Drosg 2009, p. 5).

Error

The mentioned imperfection of measurement gives rise to an error (JCGM 100:2008, p. 5) which is defined as:

> "*[The] result of a measurement minus a true value of the measurand"* (JCGM 100:2008, p. 48).

In general the goal while designing any measurement equipment or procedure is to minimize this difference between result and true value although eliminating it is not possible. The reason for this being that on one hand in practice not all sources of error can be avoided by the design of the device and on the other hand not all errors are even related to the device or measurement itself. One important thing to note is also that the actual error cannot be determined because it is a deviation from the true value which in itself cannot be known in the first place.

If a value for an error is given it is meant to be taken as *"the deviation of the best estimate from an agreed on best value"* (Drosg 2009, p. 24). JCGM notes this through stating that concerning error *"in practice a conventional true value is used"* (JCGM 100:2008, p. 36). There are different types of errors; most notably we have to differentiate between random error and systematic error shown in Figure 2.1.

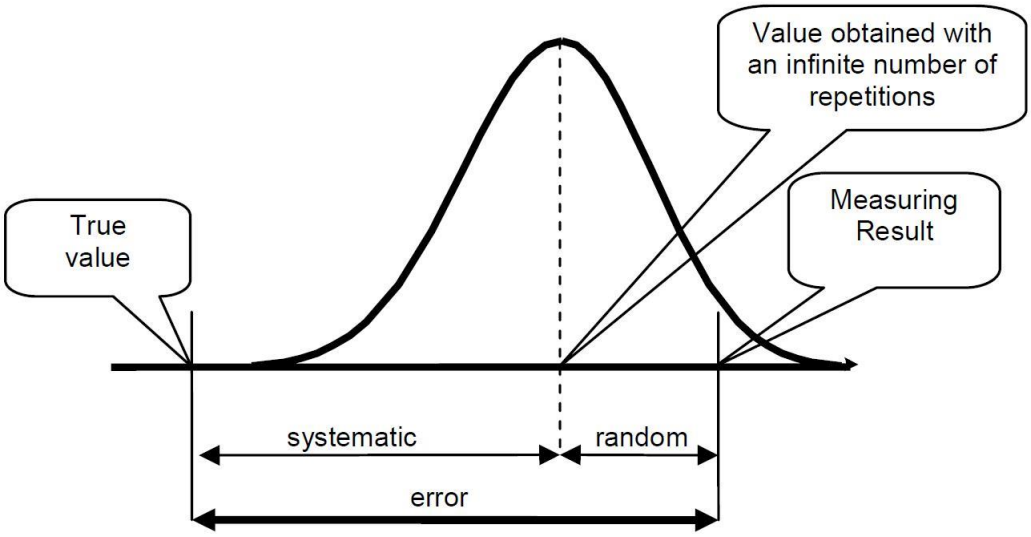

Figure 2.1: Systematic and random error (Placko 2006, p. 170)

Random error

The JCGM defines random error as:

> *"[The] result of a measurement minus the mean that would result from an infinite number of measurements of the same measurand carried out under repeatability conditions"* (JCGM 100:2008, p. 37).

Even though the Bureau International des Poids et Mesures (BIPM)/JCGM is perhaps the most important authority on measurement comparing this definition with Drosg reveals it to be not specific enough regarding the type of error. Random error cannot always be determined and counteracted by repeated measurement as not all random error is time-related (Drosg 2009, p. XI).

This can also apply to measurements carried under theoretically ideal conditions as some measurands exhibit inherently random values, for example radioactive decay. The definition given by JCGM is therefore only correct if you define random error as just those parts of the error that are random and time related.

Systematic error

> "[The] mean that would result from an infinite number of measurements of the same measurand carried out under repeatability conditions minus a true value of the measurand" (JCGM 100:2008, p. 37).

In other words the systematic error is the remaining error after you subtract the random error and the true value from the measurement. As both of these values are not and cannot be known without some uncertainty this also applies to systematic error.

Systematic error is a result of the measurement method and measurement devices used. One goal of designing a measurement device is therefore to minimize this error. Systematic error may be reduced (but not eliminated) by applying a correction or correction factor (JCGM 100:2008, p. 5).

Uncertainty

Aside from the value obtained by measuring something the uncertainty assigned to this measurement is the most important piece of information in metrological terms.

> *"[Uncertainty is] a parameter, associated with the result of a measurement, that characterizes the dispersion of the values that could reasonably be attributed to the measurand"* (JCGM 100:2008, p. 36).

As all scientifically relevant data is at least somewhat uncertain (Drosg 2009, p. 1) it is important to give not only the value obtained by measuring but also certain bounds around this value in which the true value is likely to be found with some probability. This reflects how sure someone can be that this value may be used as a practical replacement for the unknowable true value in engineering or generally scientific applications.

The function of uncertainty is therefore to give a "quasi-sure" range in which to localize the true value of a measurand (Grabe 2011, p. 4). Uncertainty is distinct from error in that it defines a range of possible values rather than a specific difference of true value and measured value. Uncertainty shows a property of the measurement in general instead of just of a singular measurement. These characteristics can be visualized as shown in Figure 2.2.

In practice uncertainty is often given in terms of standard uncertainty calculated using the following formula (Juhanko 2011, p. 71).

$$u(\bar{x}) = \sqrt{\frac{(x_1 - \bar{x})^2 + (x_2 - \bar{x})^2 + \cdots + (x_n - \bar{x})^2}{n(n-1)}} \tag{1}$$

Here $\bar{x}$ is usually the mean of the measured values which is used as the best available substitute for the true value (Dubbel et al. 2014, W 1.4.1).

In statistics terms u is known as the standard error of the mean. If u is multiplied with a coverage factor k it is an expanded standard uncertainty representing a coverage probability or in other words a probability that the true mean is within the given range. For example k=2 is equivalent to a two sided coverage probability of 95%).

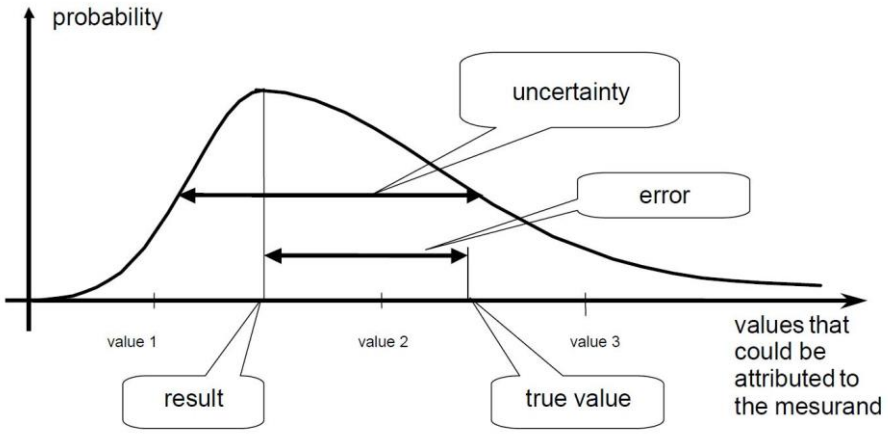

Figure 2.2: Distinction between uncertainty and error (Placko 2006, p. 165; cf. Dubbel et al. 2014, p. 5)

Principle of measurement

> *"Principles of measurement are the physical effects or laws on which the measurement is based"* (Dubbel et al. 2014, W 1.1).

A measurement may involve multiple principles especially if the sought value cannot be obtained by direct measurement. The use of these principles may introduce sources of error since the values they are based upon (for example physical constants) can also only be known with some uncertainty.

Measurement chain

> *"The general structure of a measurement system is the measurement chain composed of measurement elements and supporting devices"* (Dubbel et al. 2014, W 1.2.1).

The function of the measurement chain is to enable the practical execution of the measurement. Since every element involved in this chain can introduce uncertainty by imperfect design, imperfect manufacturing, uncertain physical properties or other reasons it is generally advisable to keep the length of this chain to a minimum.

In some cases however a trade-off needs to be made between the chain length and the usability of a measurement device. For example it might be necessary to include more elements, like an adjustment mechanism, in the device to introduce the ability to compensate for certain types of misalignments.

Trueness

> "*Trueness*" *refers to the closeness of agreement between the arithmetic mean of a large number of test results and the true or accepted reference value*." (DIN ISO 5725-1:1994, p. 9).

A very true measurement (series) would thus be one that has a very low error. Trueness in itself is not sufficient for a good measurement system, for that the measurement also needs to be repeatable.

Repeatability

> *"[The] closeness of the agreement between the results of successive measurements of the same measurand carried out under the same conditions of measurement"* (JCGM 100:2008, p. 35).

Thus repeatability makes a statement about the width of the distribution of multiple measurements taken under identical conditions. A better repeatability equals a narrower distribution but does not say anything about the trueness. Because of that good repeatability is not sufficient to determine the absolute value of a measurand.

Trueness and Repeatability combined are needed to have a measurement result that has a high probability of being close to the true value of the measurand. This is shown in Figure 2.3 where trueness is expressed in terms of freedom from bias in accordance with DIN ISO 5725. "Trueness is normally expressed in terms of bias" (DIN ISO 5725-1:1994, p. 11).

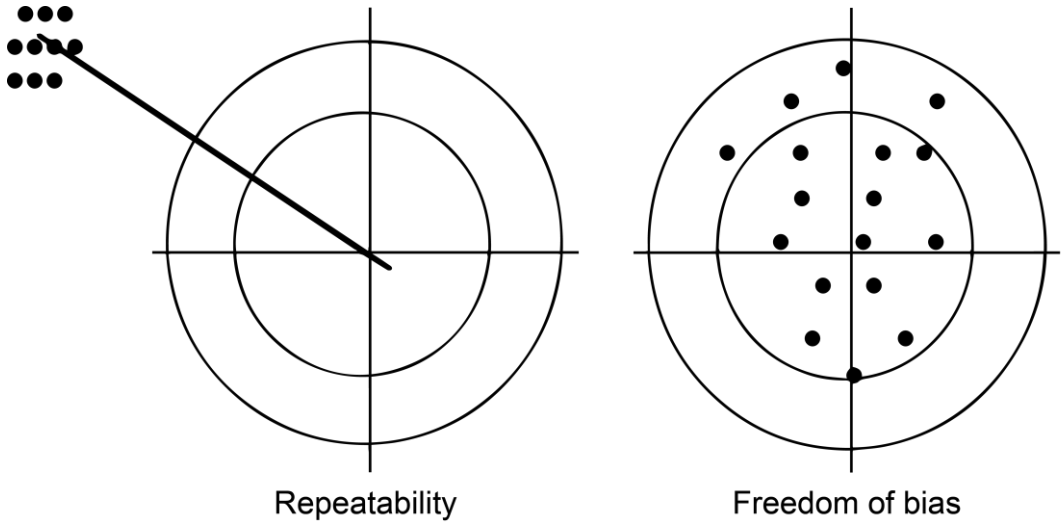

Figure 2.3: Repeatability vs. Freedom of bias (Placko 2006, p. 100)

2.2 Bearing geometry measurement

There are several standards that define the geometric properties of bearings and how they should be measured. Most notably there are DIN 620, DIN ISO 1132, ISO 199 and ISO 492. Especially relevant to this work is DIN ISO 1132-1:2001 because it defines thickness deviation for the different bearing elements.

Deviation of the thickness of the inner ring is defined as the “difference between the biggest and smallest radial distance between the bore surface and the race on the outside of the inner ring at the middle of the race” (DIN ISO 1132-1, p. 15). It has to be noted that the middle of the race can lie in different positions on the bearing as it is dependent on the bearing and race geometry. In some cases the contact point of the rolling elements might also not be in the middle of the race, in this case the standardized geometric specification does not change but measuring the thickness deviation at different points can be beneficial to determining the actual bearing quality.

The standard also notes that the radial accuracy of a bearing is a result of multiple factors (DIN ISO 1132-1, p. 16) but it does not list those factors. The focus of the standard is defining the geometry of the bearing itself but it does not account for the running parameters of a mounted bearing that are influenced by these factors which this work focuses on.

DIN 620-1:1982 defines how the thickness deviation should be measured but it only gives a rough idea of the measurement setup and process. Figure 2.4 shows the described setup consisting of a measurement instrument and two gliding surfaces that the bearing rests against. This setup is targeted at manual measurement which requires more effort while measuring multiple rounds. This kind of manual measurement is also hard to implement with large scale bearing elements as their mass alone makes manual movement difficult. The standard however explicitly allows for alternate measurement methods (DIN 620-1, p. 2).

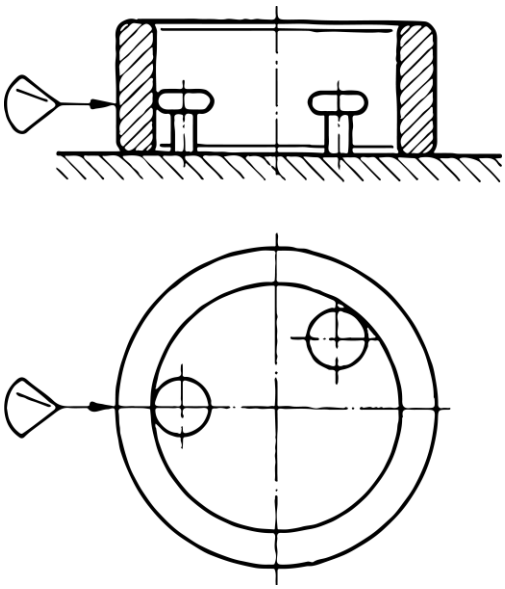

Figure 2.4: Standardized bearing ring thickness measurement setup (DIN 620-1, p. 4)

2.3 Existing devices

The most common measurement principle used to measure the components that this thesis focuses on is indirect optical measurement via a tactile sensor. The geometry of the part is transferred to the actual sensor via a tactile probe that is guided along the surface of the part.

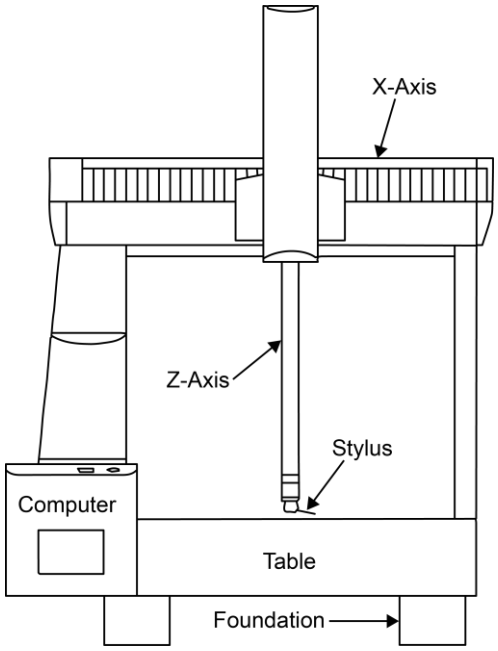

Figure 2.5: Layout of a coordinate measurement machine (based on Mitutoyo 2013, p. 6)

There are two common types of devices, coordinate measurement machines and more specialized roundness measurement machines. In case of the first any point within the coordinate space of the device can be reached by the probe (although the measured part itself might block access to some points) and the surface of the part can thereby be probed on a point by point basis. In case of the second the part rotates on a table so that measurements can be taken all around its outer or inner circumference.

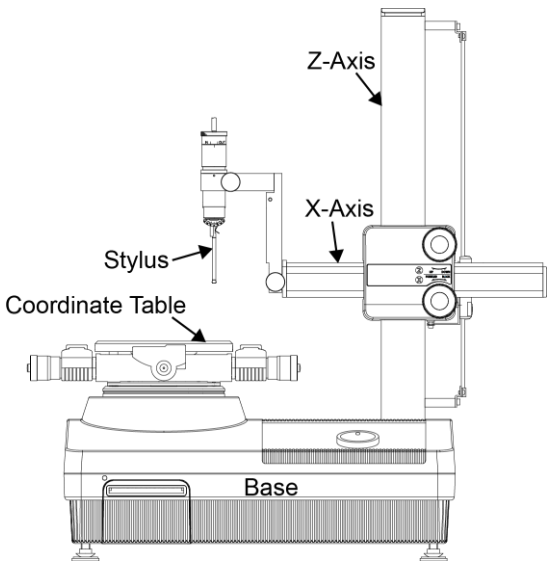

Figure 2.6: Layout of a roundness measurement machine (based on Mitutoyo 2014b, p. 11)

The benefit of this method is that it is usually faster and somewhat more accurate, while the drawback is that it can only be used for round components. If the component is a ring the measurement process is then either repeated on the inside of the component. Alternatively dual probes would need to be used. In case of dual probes the thickness could be directly determined via the difference between these two measurements. The benefit of this is that realignment of the part or sensors between the inner and outer measurement can be avoided and the data acquisition rate is effectively doubled as two measurements are taken concurrently. Also the length of the measurement chain between the two sensors can be very short and as such should result in a higher accuracy. Galyer and Shotbolt note that “only by the application of kinematic principles can the design of an instrument or machine be such that its accuracy in operation does not rest entirely on its accuracy of manufacture” (Galyer, Shotbolt 1990, p. 47). With differential measurement this is realized because the absolute movement of the bearing during measurement and the roundness component are automatically removed by the coupled movement of the two tactile probes.

2.3.1 Existing prototype

As part of a previous project a prototype (shown in Figure 2.7) for a new design was made. That device was used in for this work as a basis for further improvement. The mode of operation of this prototype is as follows.

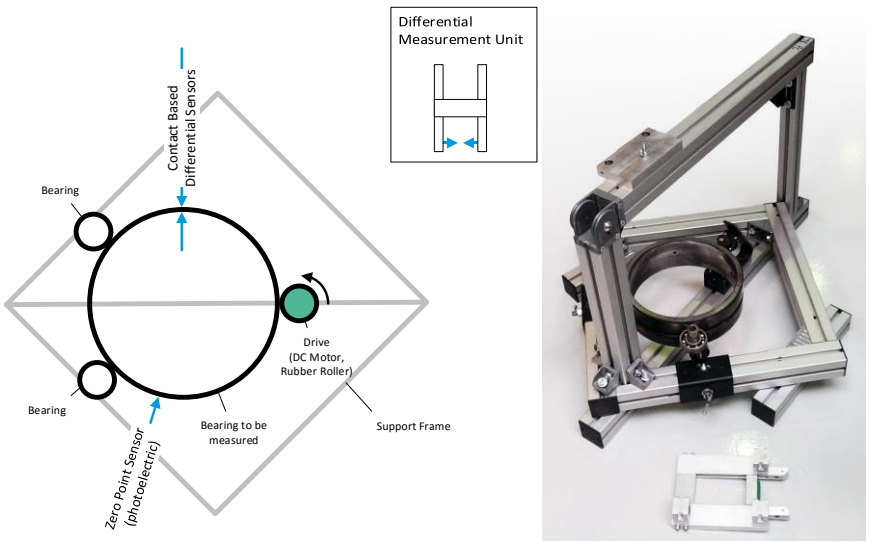

Figure 2.7: Operating principle (schematic top view) and photograph of previous prototype

The bearing element under test is placed into the device and adjusted by two sliding elements that contain ball bearings on which the bearing rests upon or against. The bearing is then rotated via a friction wheel driven by a DC motor which is placed on a third sliding element. This element also acts as a clamping device pressing the bearing under test against the support bearings. The prototype was originally meant to be angled relative to the ground so that this function is achieved via gravity, however due to the flexibility of the motor mount and the rubber drive wheel this is not necessary.

While the bearing rotates the thickness is continually measured with two tactile length gauges. These two sensors are mounted to a measurement head or fork guided by two rods suspended from the upper cross member of the devices frame. The fork contains a plastic gliding surface which rests upon the top surface of the bearing. The gliding surface is adjustable in the vertical direction relative to the sensors. Consequently the top surface of the bearing acts as the vertical reference for the measurement or in other words the measurement is taken at a certain distance from the bearings upper surface.

The use of two sensors connected directly by the fork enables differential measurement in contrast to having to measure the inside and outside of the ring separately. This is one of the main differences that separate the prototype design from conventional designs described before. This approach theoretically shortens the measurement chain necessary for measuring the thickness to only the sensors themselves and the fork connecting them, possibly improving the quality of measurement and/or making the device cheaper compared to traditional devices. However the chain is not always limited to the measurement head itself here since the alignment between the bearing and the sensors also depends on the frame of the device.

Initial testing with this prototype device revealed a couple of flaws that are not inherent to the concept itself but rather to the design of the prototype. Due to big tolerances in the vertical guidance system and the sensor head geometry, probe springs and the tribological properties of the contact between the probes and the bearing element there are some resonance issues that occur in repeating but not reliably repeatable patterns.

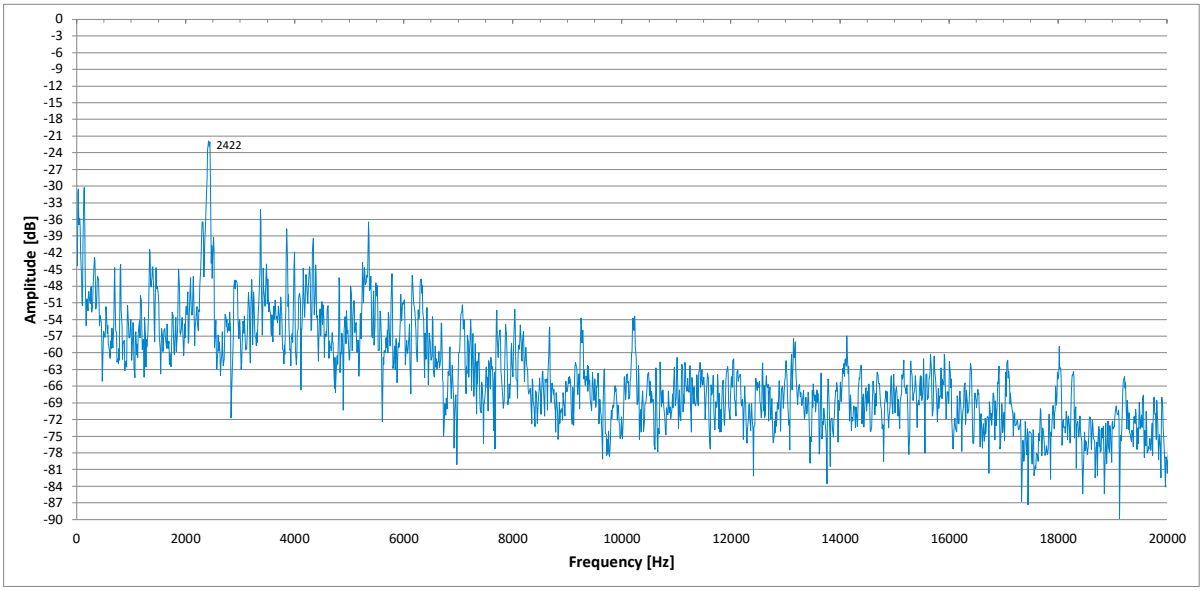

Figure 2.8: FFT spectrum showing prototype device vibration

Because the vibration frequency is to high to detect in a fast Fourier transformation (FFT) spectrum generated from the measurement data itself but is clearly hearable the resonance frequency can be determined via an audio recording. The spectrum resulting from this is depicted in Figure 2.8.

The main frequency of 2.4 kHz is at the upper limit of what could be detected with the sensors themselves through the IK220 measurement card using its maximum sampling rate but it is much more feasible to use standard audio equipment to do this. Although this resonance phenomenon is certainly an issue it is possible to collect enough data that does not exhibit this problem because it only occurs randomly from time to time.

A more problematic issue with the design of the machine is that the vertical axis is defined by a gliding surface of which the vertical distance to the sensors cannot be precisely adjusted because there is no proper adjustment mechanism. The gliding surface is moved by unfastening and refastening it from/to the fork and it does not feature any kind of scale which makes good adjustment accuracy not realistically achievable. The gliding surface is also made from a plastic compound which shows signs of wear even after only a short usage period, this means that measurements that are taken at a set height are not repeatable for many cycles on the same machine even without changing the height.

Another problem with setting up the machine is that the direction that the support bearings are moving in is rotated 45° to the coordinate system of the measurement head and the guide mechanism clearances are not small enough. The 45° rotation means that both of the guides have to be moved at the same time to move the bearing under test in the direction perpendicular to the sensor probes. At the same time great care has to be taken not to push the bearing ring of the third support bearing (at the motor side) while moving the other two supports. This kind of movement is necessary for finding the minimum thickness and therefore the point where the axis connecting the sensor probes goes through the centre of the circle. In practice adjusting the minimum to less than 20 μm is very hard to achieve. Because of this the absolute trueness of the device is compromised.

Initial measurement data shows several artefacts resulting from the measurement device and process. To obtain absolute thickness values for this dataset a calibration block was used and the bearing element (outer ring of a spherical roller bearing FAG 23134, see Schaeffler 2016) was then measured 10 times with a sampling rate of 100 Hz, lifting and resetting the sensor head after 5 repetitions.

As accurately setting the height on this prototype is not possible it was set to an arbitrary position near the middle of the race. This dataset can therefore not be used to compare absolute thickness results between the prototype and the device constructed for this thesis but it can be used to analyse the repeatability of measurements in regard to multiple measurement objectives. These repeatability values can then be used to compare the old prototype to the newer device (see chapter 4).

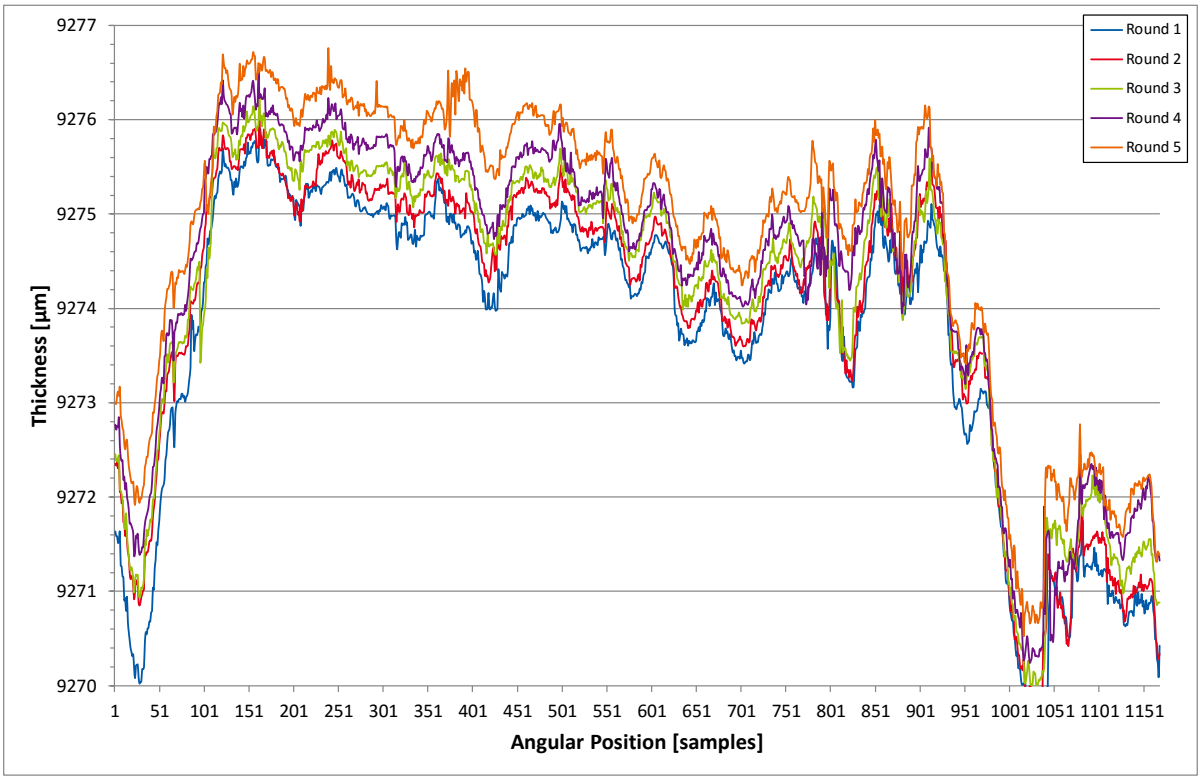

Figure 2.9: Bearing thickness measured with previous prototype

Figure 2.9 shows a noticeable drift between successive repetitions. The change in measured mean thickness between the first and fifth repetition is about 1.0 μm. The change between the sixth and tenth repletion shows a similar change of 0.9 μm. One possible explanation for this is the clearance in the guiding system of the device which leads to varying misalignments in multiple directions.

The differences between the mean values before and after lifting the measurement head are much larger at 28.8 μm. This fits well with the assumption that these changes are due to the play in the mechanism because manually moving the head influences the position within the given clearance.

Aside from the absolute thickness we can look at the thickness deviation within one round, as previously stated this factor is important to the run-out of the assembled bearing. If we look at the thickness variation obtainable by calculating the difference between the minimum and maximum thickness measured during one rotation the results appear to be consistent between consecutive rounds as well as after manual interaction with the device.

Figure 2.10 shows the thickness deviation for all 10 repetitions. The maximum difference for these values is 0.4 μm which is in the same range as the system accuracy of the used sensors (see Heidenhain 2013, p. 4).

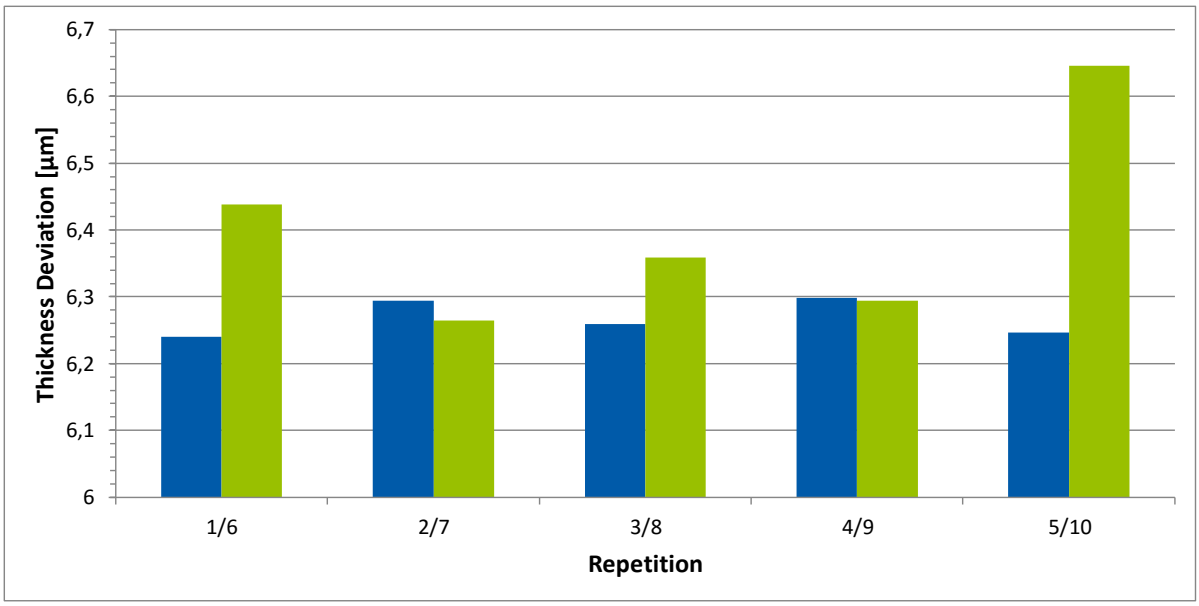

Figure 2.10: Comparison of thickness deviation before and after manual interaction

A change in the range of 30 μm even between measurements taken in short succession and without changing the measurement environment already demonstrates that the prototype device is not suitable for obtaining a good estimate of the true absolute thickness. However the repeatability for the thickness deviation is already very good compared to what the sensors are capable of.

Setup time and absolute value calibration as well as the vibration problems mentioned before are the main weak points of this design. These issues are addressed in the new device that was made as part of this work and the changes that were made in this regard are detailed in chapter 3.2.

3 Materials and methods

3.1 Concept

In the following chapters different concepts for a measurement device design are presented, compared and evaluated. The pros and cons of the various options are then discussed and the decision process and the chosen concept are explained in detail.

3.1.1 Morphological Box

To come up with new design concepts for this project a well-known creativity technique was used. The morphological box works by dividing a concept into different abstract categories or attributes. For each category you then find different possible values. By then finding all possible combinations of values for each attribute new concepts can be found that may not have been obvious by just trying to think of new concepts.

In this case the following attributes and values were chosen after analysing the older prototype of the device and identifying its main components.

- Moving
    - Bearing: The bearing is moved/rotated in the device
    - Device: The device itself moves around the bearing
- Anchor (only applies to moving device)
    - None: The moving device is not referenced to a stationary external reference
    - Reference: The moving device is referenced to an external reference
- Movement relative to anchor (only applies to moving device)
    - Not applicable: No anchor or no moving device
    - Rotation: The device only does rotational movement relative to the reference
    - Rotation/Translation: The device does rotational and/or translational movement relative to the reference
- Measurement degrees of freedom
    - 1, 2, 3, 4: The possible degrees of freedom of movement a given device has by design during operation

- Movement measurement
    - None: The movement is not measured, only the thickness is recorded
    - Zero Point: A reference mark is added to detect every full rotation
    - Relative: An encoder is used to monitor the movement
    - Zero Point + Relative: Both a reference mark and an encoder are used
    - Absolute: An absolute scale is added to track the movement
- Motion Coupling
    - Static Friction: The moving element is driven by static friction (for example a bearing sitting on a rotatory table)
    - Rolling Friction: The moving element is driven by rolling friction
    - Fastening: The moving element is fastened to the driving system

The resulting morphological box is shown in Table 3.1 including one exemplary alternative device concept, the concept of the existing prototype and the concept of the new device (green). While a morphological box is regularly made using symbols it is represented here in a textualized version to make it easier to understand without explaining the pictograms used.

Moving	Device	Bearing			
Anchor	Reference	None			
Movement relative to anchor	N/A	Rotation	Rotation + Translation		
Measurement DoF	1	2	3	4	5
Measurement Process	2-Stage	Differential			
Movement Measurement	None	Zero Point	Relative	Zero Point + Relative	Absolute
Motion Coupling	Static Friction	Rolling Friction	Fastening		

Table 3.1: Morphological box for device concepts (Blue: Prototype, Green: Alternative 1, Yellow: Alternative 2)

For the measurement process all concepts that were considered for the new prototype employ the differential setup because the differential measurement head is one of the main differentiating factors between this work and conventional bearing measurement machines that should allow for the desired improvements described in subchapter 1.2.

Figure 3.1 shows two examples of moving device style designs. The design on the right features a central reference point with a frame that extends to the cart that rides on the bearing element itself. This would allow for angular encoding using a rotary encoder on a central shaft. Because the gearing ratio between the device rotation and the encoder can be 1:1 without any additional gearing correlating the thickness values to the encoder signal can easily be accomplished. This would improve the angular mapping repeatability across multiple measured rounds.

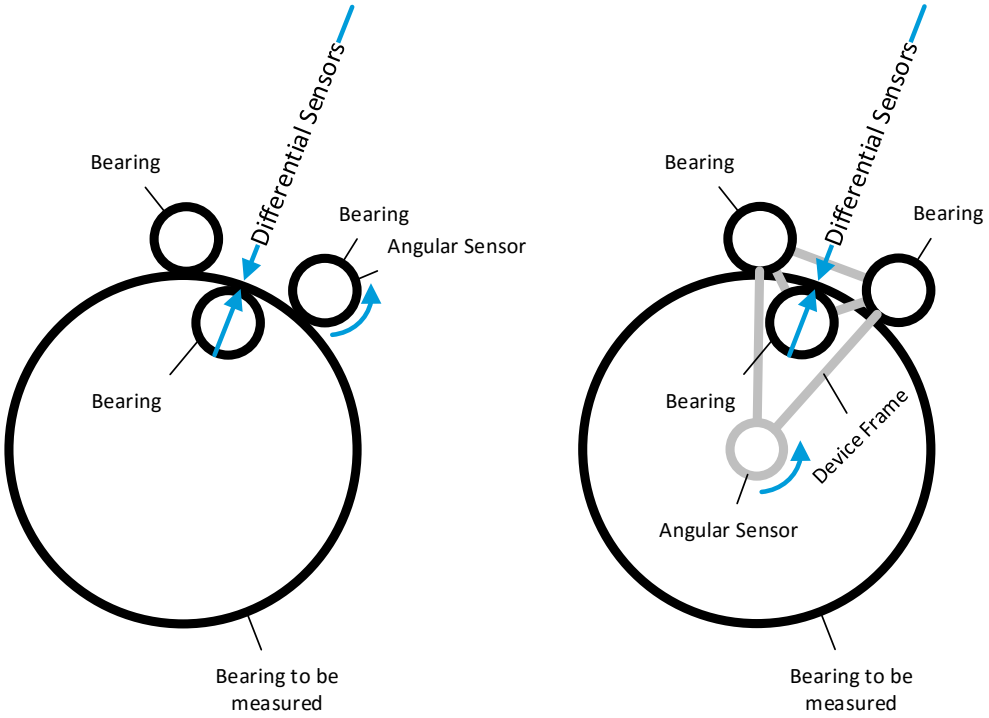

Figure 3.1: Moving device style concepts (Schematic top view)

A challenge with this design is centring the reference point relative to the bearing. Misalignment would require the sensor head to moveable in the radial direction. While this can easily be achieved in terms of kinematics it would lead to a misrepresentation of the sensors circumferential position because its relation to the angular position would no longer be constant. While consecutive rounds would still produce similar results reproducing these across multiple measurement sessions would need the central reference point to be in exactly the same position for both measurements.

In Figure 3.2 two examples for moving bearing devices are given. The left one includes a chuck comparable to one that could be found on a lathe while the other one relies on static friction between a rotating table and the bearing (compare Table 3.1).

These configurations also allow for the usage of a central rotary encoder that is directly coupled to the bearing rotation. Like the moving device concept without any central reference point the turn table design exhibits the same issue of needing to be centred. The design utilizing a jaw chuck does not have this problem but the chuck mechanism itself needs to be manufactured very precisely to prevent any misaligned of the centre of rotation.

Because the bearing rests upon the rotating part of these devices the mechanics and possibly also the drivetrain need to be able to support the weight of the bearing element without excessive deformation which likewise increases the design and manufacturing complexity.

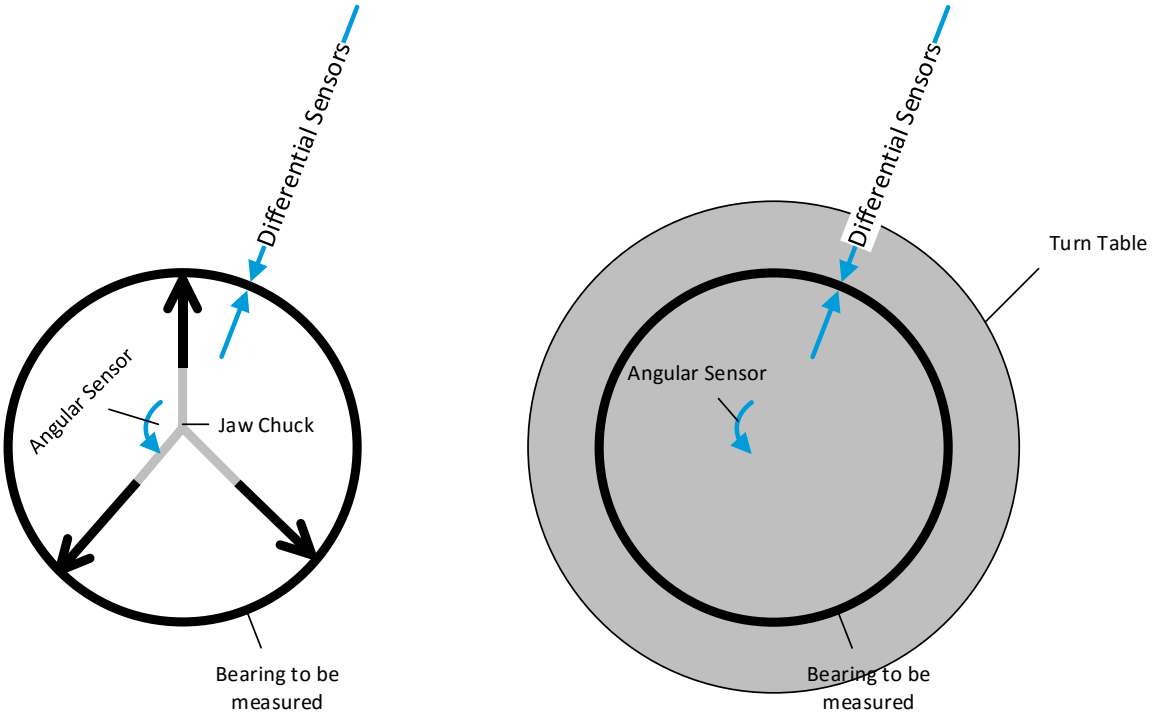

Figure 3.2: Moving bearing style concepts (schematic top view)

Aside from the concepts explained so far the possibility of making a device capable of measuring the thickness of the rings without disassembling the bearing was evaluated. This would offer significant benefits especially for inspection and maintenance applications. To make this possible very thin and long thickness measurement probes would be necessary as they need to be able to fit in-between the rolling elements and potentially the bearing cage. To investigate this concept computer models of the sensors where tried on different bearing models in the given size range.

Tactile probes that measure parallel to their axis of movement are not suitable for this application because the clearance between the bearing components is smaller than the available sensors. Probes that measure perpendicular to their direction of movement such as the ones used on contour measurement machines would require very long styli which would be challenging in execution. These sensors also rely on gravity to keep contact with the surface they are measuring. That would require the bearing to be in an upright position which would make handling it difficult.

Confocal optical sensors that also measure perpendicular to their longitudinal axis are available but only offer a measuring range in the same magnitude as their own thickness (Micro-Epsilon 2015, p. 7). This would necessitate adjustability of the sensor mount with several degrees of freedom as the tip of the sensor always needs to be close to the measured surface. This adjustability leads to the problem of keeping the sensor outside the bearing and the sensor inside the bearing aligned with each other. In summary no sensors seem to be available that would make the implementation of such a design feasible at this point in time.

The principle of the morphological box can also be applied to less abstract parts of the design such as the different possible component choices. As the meaning of the different possible values for every attribute is more obvious in this case because of the more tangible nature they will not be explained to the same level of detail. However it should be noted that after a market survey was done only the technologies that are actually applicable for this task were included. The morphological box for the actual components can be seen in Table 3.2.

Motor	AC	DC	Servo	Stepper	
Thickness Sensor	Tactile	Optical	Ultrasonic	Electromagnetic	Radiometric
Zero Point Sensor	Electromagnetic	Optical	None		
Rotation Sensor	Rotary Encoder	Optical	None		

Table 3.2: Morphological box for device components

For this application tactile sensors offer the best resolution and accuracy while being usable regardless of other attributes of the components to be measured. For example surface reflectivity might interfere with optical sensors while inhomogeneous magnetic properties can influence electromagnetic sensors such as eddy current sensors. DC Motors were chosen as they are readily available for the given power and speed range and offer good controllability as well as low electromagnetic interference emissions. For the rotational sensing rotary encoders are the industry standard and offer the additional benefit of being compatible with the same data acquisition interface as the tactile length gauges used in this work. Because of this correlation between the thickness signal and angular position signal can easily be obtained by linking the measurement cards.

3.1.2 Sensor head concept

As part of the conceptual design phase the differential sensor head at the core of the device design was also looked at. While the previous generation prototype employs two sensors directly opposing each other a more specialized design was thought up. The goal of that alternative design was to take the known overall shape of the bearing elements into account to mathematically remove errors resulting from misalignment of the head in relation to the rest of the device and the bearing element under test.

Either the outer or inner circumference of a standard bearing element can be approximated by a cylinder shape. The opposing surface is either also cylindrical (for cylindrical roller bearing) or spherical (for spherical roller bearings and ball bearings). Although there are various other types of bearing elements these types are of special interest as they are the most common for very large scale bearings.

If we look at a cut through a bearing element (see Figure 3.3), in this case a spherical roller bearing, we can see that the cylindrical surface (side A) maps to a straight line while the spherical surface (side B) maps to a partial circle. The current approach would only use two opposing sensors (for example A1 and B1) to determine the thickness.

Alternatively the 5 sensor approach would calculate the 2 mentioned geometric primitives based on 2 (line) respective 3 (circle) points. As the current test specimen is of the spherical type the following calculations will be based on that geometry, as the cylindrical geometry is simpler in terms of calculating the thickness. In that case one of the sensors on side B could be discarded while measuring cylindrical roller bearings. These 2D representations of the bearing could then theoretically be used to generate a thickness profile while measuring all around the bearing.

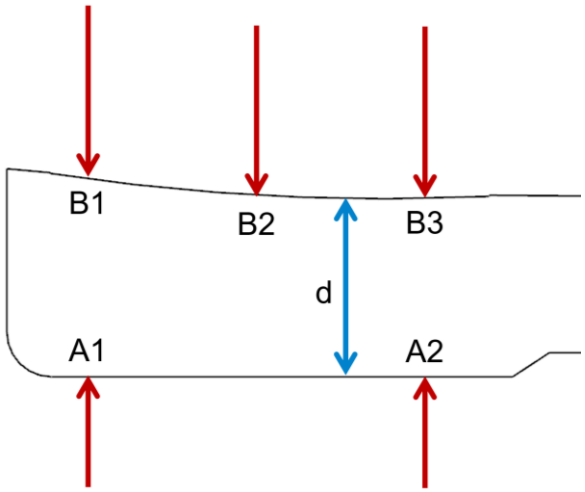

Figure 3.3: Partial cross section of a spherical roller bearing

3.1.3 Sensitivity Analysis

To evaluate the feasibility and expected accuracy of the different sensor head concepts the geometry of the two options was analysed in order to investigate the sensitivity to different possible misalignments or unintentional movements.

The sensitivity analysis process consists of two steps:

1. Finding an equation that translates the movement of the probes into the sought thickness
2. Finding a set of equations that translates the sensor head misalignment into the movement of the tactile probes

In case of the 2 sensor solution the first step is trivial as the thickness is directly given by the addition of the 2 sensor values. Contrary to that the geometry of the 5 sensor solution makes the first step more elaborate as will be demonstrated below.

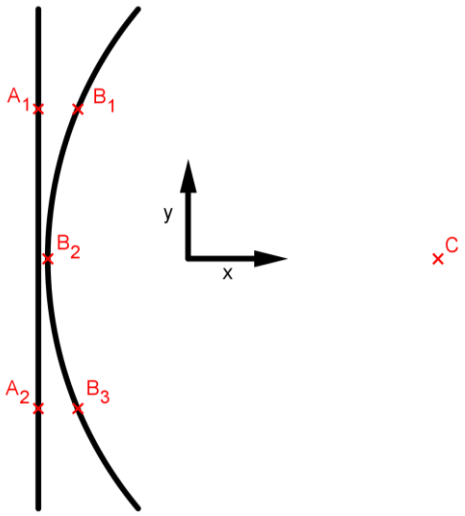

Figure 3.4: Simplified bearing wall geometry with coordinate system

To determine the thickness of a given element placed between the 5 sensors we need to find the line L that connects the 2 points A1 and A2 (see Figure 3.4) as well as the circle that is defined by the 3 points B1, B2 and B3. The coordinates of those points will further be denoted as $A1_x$, $A1_y$, et cetera. Using the coordinate system shown in Figure 3.4 the line is given by (2).

$$y_s = x\frac{A1_y - A2_y}{A1_x - A2_x} \tag{2}$$

For the circle we need to determine its centre as well as its radius. The centre point can be obtained by constructing two lines that are both perpendicular to one of the lines connecting point B1, B2 and B3, B2.

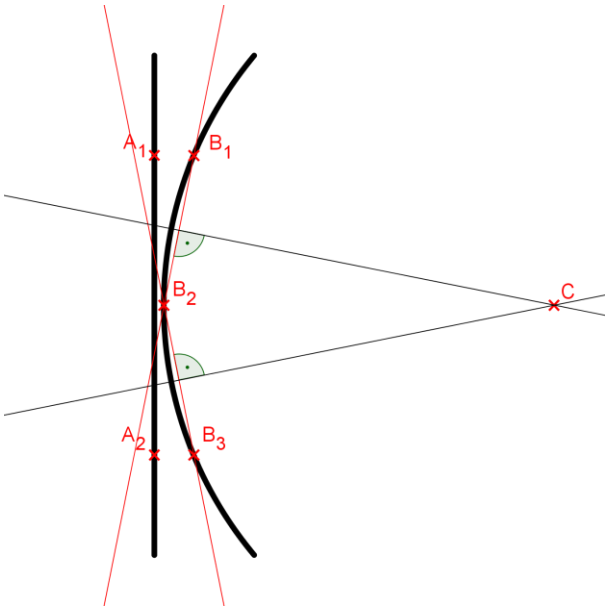

Figure 3.5: Finding the centre of a circle defined by three points

Analogous to (2) these lines are described by (3).

$$y_i = x\frac{B1_y - B2_y}{B1_x - B2_x};\ i = \{1,3\} \tag{3}$$

The intersection point of those lines C is the centre of the circle whose coordinates can be found through (4) and (5) (Roberts 2012).

$$C_x = \frac{y_1 y_3(B3_y - B1_y) + y_1(B2_x + B3_x) - y_3(B1_x + B2_x)}{2(y_1 - y_3)} \tag{4}$$

$$C_y = \frac{B2_y + B3_y}{2} - \frac{1}{y_3}(C_x - \frac{B2_x + B3_x}{2}) \tag{5}$$

The radius of the circle can be obtained by applying the Pythagorean theorem for any point on the circle, in this case B1, B2 or B3, and the centre point C resulting in (6).

$$r = \sqrt{(Bj_x - C_x)^2 + (Bj_y - C_y)^2};j = \{1,2,3\} \tag{6}$$

If we now define the thickness as the shortest distance between the line L and the circle we have constructed we can find that value based on calculating the distance between the line and the centre point and consecutively subtracting the radius. This can be seen in Figure 3.6.

The shortest distance between the line and the centre point is necessarily perpendicular to the line. We can find that by calculating the horizontal distance between the centre and the line and the angle of the line L to the x direction. The horizontal distance h is given by entering C_y into (2), subtracting the result from C_x yields (7). While the angle β can be found as per (8).

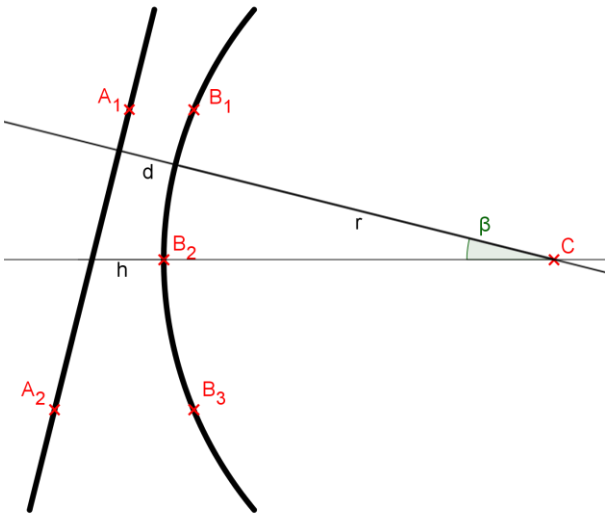

Figure 3.6: Thickness calculation using simplified geometry

$$h = C_x - C_y \frac{A1_x - A2_x}{A1_y - A2_y} \tag{7}$$

$$\beta = \tan^{-1}\left(\frac{A1_y - A2_y}{A1_x - A2_x}\right) \tag{8}$$

The sought thickness or minimal distance d is finally obtained as (9).

$$d = h\sin(\beta) - r \tag{9}$$

Although these steps are not complex on their own the resulting equation, which is not shown here for sake of brevity (see appendix), makes algebraic sensitivity analysis via partial derivation non trivial. The partial derivatives that can be obtained with a computer algebra system do not offer any intuitive insight as to which changes the system would be most sensitive to.

Looking at the resulting thickness over different input parameters while keeping the other parameters constant can be helpful for understanding the behaviour of the system. For example it is obvious that the measured thickness will not change if B_{1x} and B_{3x} change but stay equal as long as the line A_1 A_2 stays vertical. This is because in this case the thickness is only defined by the difference between A_{1x} respectively A_{2x} and $B_{2x.}$ Such insights can be found through only looking at the geometry and without needing the equations but they cannot cover every possible combination of inputs as the problem is inherently multi-dimensional.

The shown complexity of the 5 sensor system is not desirable in a measurement device as it complicates analysis and therefore does not achieve the original design goal of error separation. There are also some practical aspects that make the 5 sensor design unsuitable for this application. The initial assumption that 1 side of the bearing has a circular shape turns out to be invalid. Bearing manufacturers use different shapes in this application and as these are usually kept as a trade secret it is not possible to determine if a comparable geometric approach using not more than 3 sensors on one side would be possible.

Even if that would be the case measuring the bearing elements might also be done to check for wear on the bearing surfaces. If there is some wear to the surface any assumptions made based on the original bearing geometry are consequently invalid. Using those assumptions while measuring a worn bearing would henceforth lead to false measurement results. As a conclusion of this first analysis step the design utilizing 5 tactile probes was discarded as it was deemed unsuitable for the given task.

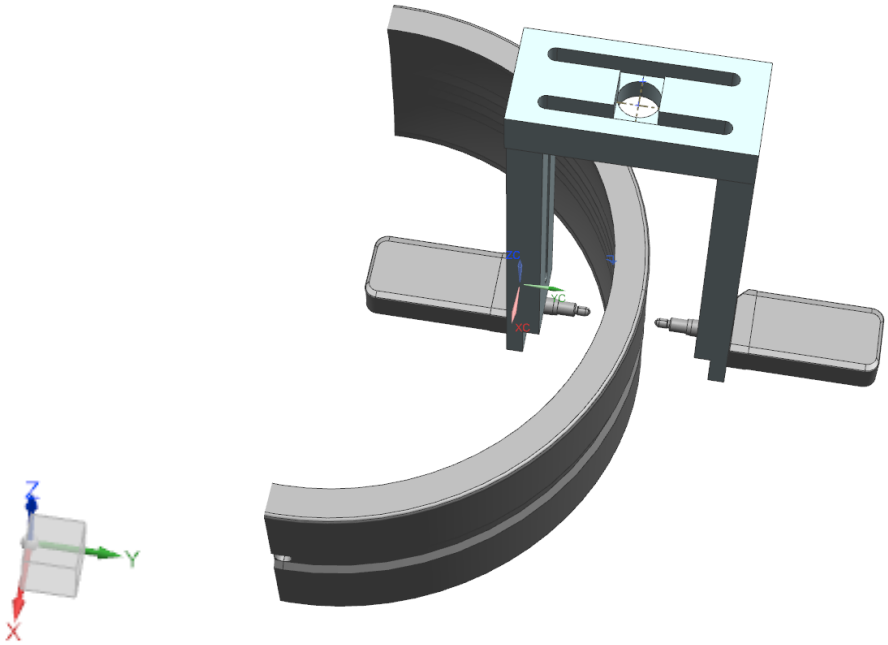

Figure 3.7: Measurement head and bearing element (cut) with coordinate system

The second step can be divided into multiple subtasks for each degree of freedom that the measurement head has around the bearing. To better understand these different movements and directions Figure 3.7 shows a version of the measurement head and a bearing element as well as the coordinate system used here.

The measurement result is independent from the movement in some directions such as rotation or translation around, respectively along the probe movement axis (parallel to Y) so these directions will not be examined further. Even though it was already noted that the actual bearing geometry is not strictly circular this simplification is still used here as it is a useful general approximation to estimate the resulting errors.

If we look at the movement of the sensor head along the height axis (Z) (see Figure 3.7) parallel to the straight inner or outer surface of the element to be measured we can see that one sensor again follows a circular path while the opposing one follows a straight line. The change in thickness therefore is dependent on the major bearing radius R_i as well as the radius of the rolling surface R_c and the height offset o_z. Because the desired initial measurement position (without any unwanted offset) might not be at the same height as the centre of the bearing a two stepped approach is necessary, this is visualized in Figure 3.8.

First we calculate the thickness at a given height h_m and then we compare it to the thickness at that height plus the offset o_z. The measurement height is equal to the sinus between the line which connects the centre of the bearing and the Y-axis as denoted in (10).

$$\sin \alpha = \frac{h_m}{R_c} \tag{10}$$

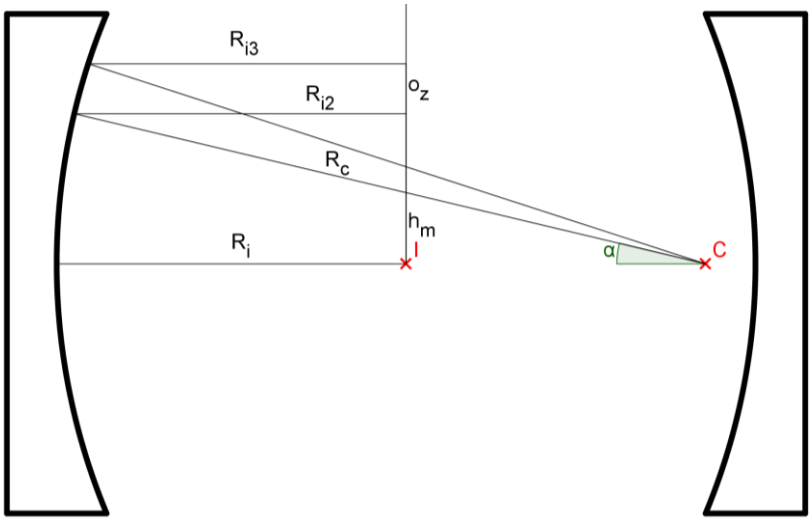

Figure 3.8: Determining thickness change from height offset

The Y position of the sensor R_{i3} at the height h_m+o_z can then be calculated as shown in (11), while R_{i2} would be the sensor position without the offset.

$$R_{i3} = R_i - R_c\left(1 - \cos\left(\sin^{-1}\left(\frac{h_m + o_z}{R_c}\right)\right)\right) \tag{11}$$

This also gives us the thickness change without looking at the movement of the opposing sensor as the Z direction is parallel to the straight outer bearing surface and perpendicular to the sensor axis. Therefor this motion does not lead to any change in the value measured by the second sensor. The sought thickness change is then given by (12).

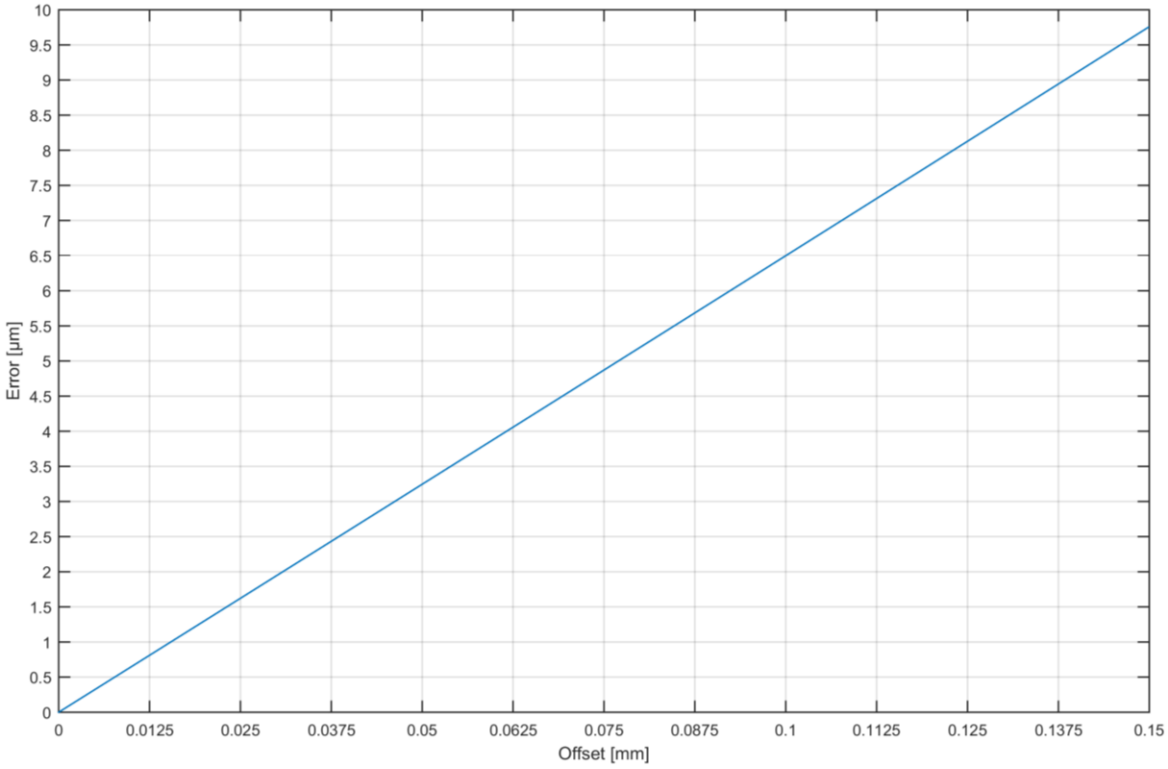

Figure 3.9: Resulting error over height offset

$$\Delta d_1 = R_{i2} - R_{i3} \tag{12}$$

Plotting this equation (see Figure 3.9) we can see that on the scale the device is intended to measure the resulting error appears linear however this is not the case for global shape of the function. The device is not very sensitive to height offsets as long as the desired measurement position is not too far from the thinnest point of the race.

In bearings where the surface radius of the race is large even big height offsets do not lead to large errors however for stronger curvatures the height offset becomes more important. This is demonstrates that the quality of the measurements obtained by the device are not only dependent on the device itself but also on what specific bearing is measured.

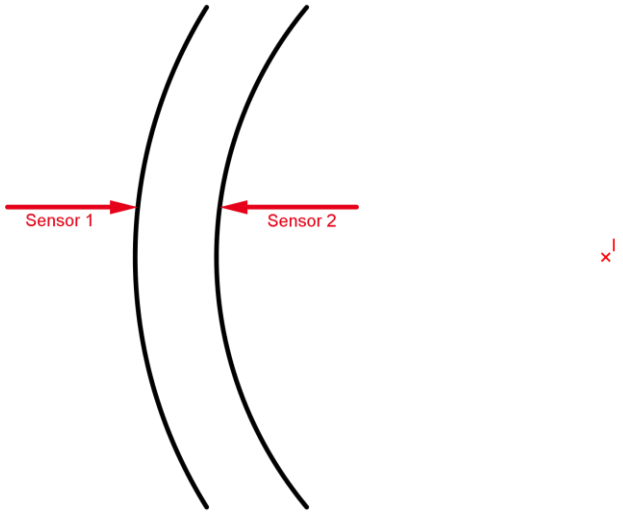

Figure 3.10: Simplified representation of two sensor layout projected onto XY-Plane

The other translational movement that is relevant here is along the X-axis. Here both sensors follow along a circular path as the projection of the bearing onto the X-Y plane, shown in Figure 3.10, is a ring. The initial thickness is the thickness at a given height d_1 that we calculated before. We also need the outer radius of the bearing R_o and the new inner radius R_{i3}. The angles between the Y-axis and the inner/outer contact points are α_i and α_o. The resulting thickness d_2 is shown in (13).

$$d_2 = R_o \cos\left(\sin^{-1}\left(\frac{o_x}{R_o}\right)\right) - R_{i3} \cos\left(\sin^{-1}\left(\frac{o_x}{R_{i3}}\right)\right) \tag{13}$$

From this we can determine that for an offset in the X direction of 0.15 mm the expected error is only approximately 1 μm. In other words this means the error resulting from this offset alone is very small when compared to the other possible misalignments. The reason for this is that unlike in the previous case both sensors move on a circle and therefore the relative movement between them is small.

Now besides the translational movement we also need to consider the rotational movement. The pole that the device rotates around is defined here as the contact point on the bearings top surface, this is because the top surface was defined as the height reference and the previous prototype as well as some of the concepts rest upon it.

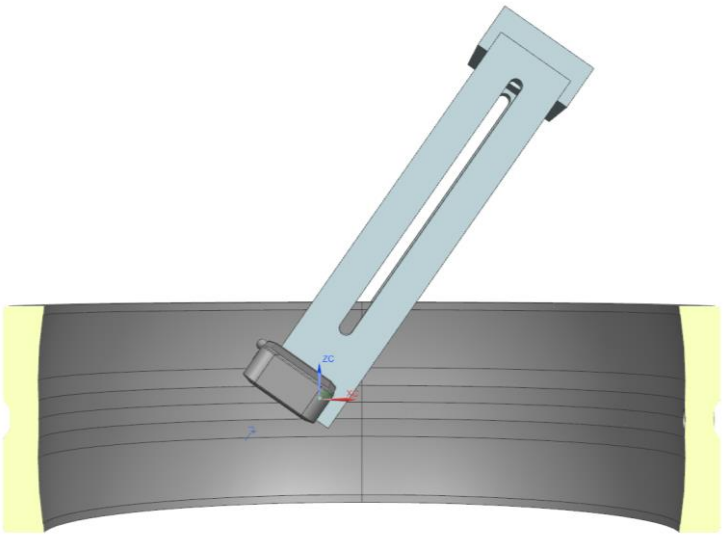

Figure 3.11: Tilting the sensor head around the Y-axis

Here the angle γ is the angle between the Z-axis and the vertical direction of the sensor fork. A rotation around the resting pole (see Figure 3.11) causes a combination of the previously determined movements of the sensors in the X and Z direction. The offset in the X direction can be calculated from the Z distance between the top surface and the sensors h_m and γ as shown in (14).

$$o_x = h_m \sin(\gamma) \tag{14}$$

Analogous the Y offset can be determined using (15).

$$o_y = h_m\big(1 - \cos(\gamma)\big) \tag{15}$$

These offsets are then consecutively used to calculate R_{i3} using (11) and d_2 using (13). We can then plot the result over γ. From the graph shown in Figure 3.12 we can deduct that tilting of the measurement head in the Y-axis around the top surface leads to errors that are bigger than the pure height offset errors. This makes sense because the errors resulting from height offset and X-axis offset both carry the same sign.

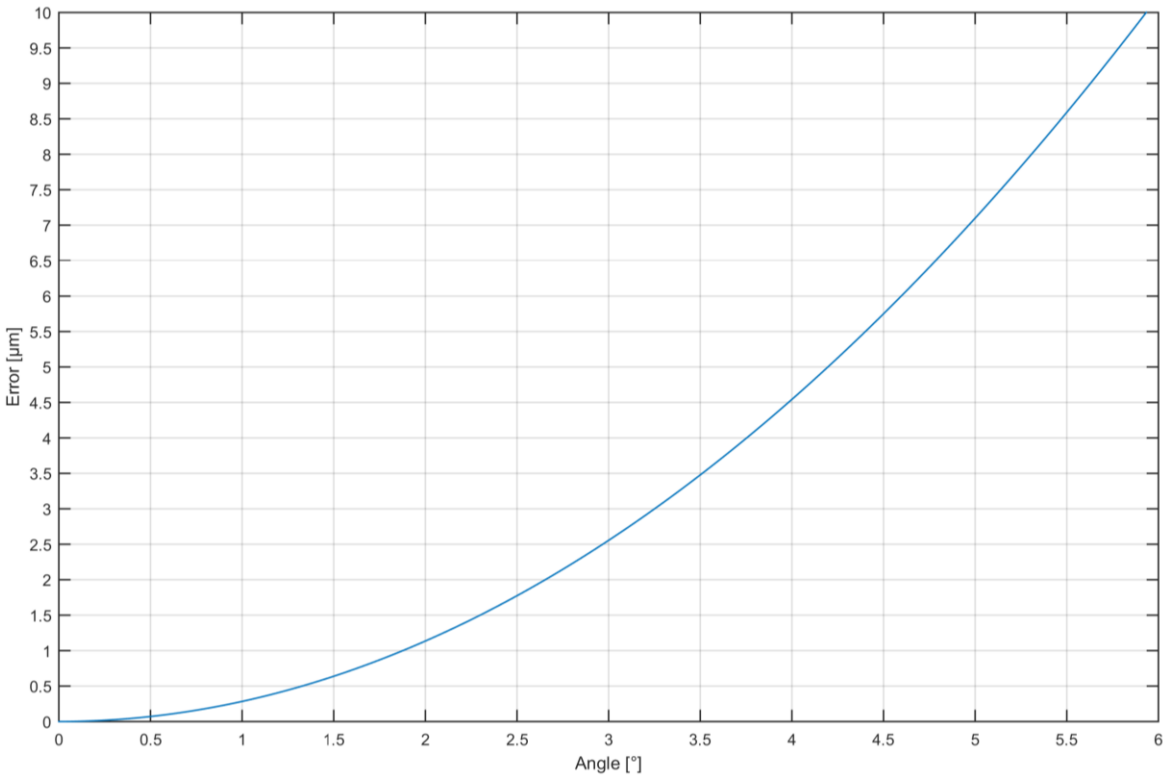

Figure 3.12: Resulting error over tilting angle (Y-Axis)

Additionally the leverage between the stationary pole and the sensors plays a deciding role because it amplifies even small angular offsets. Therefore contrary to pure height offsets the system becomes more sensitive to these errors when the distance at which the thickness is measured is further apart from the top surface of the bearing. Finally we need to look at the rotation around the X axis. Here the contact points once more follow either the curved or straight surface but they are no longer at the same Z level which causes the measured thickness to be a diagonal across the bearing section.

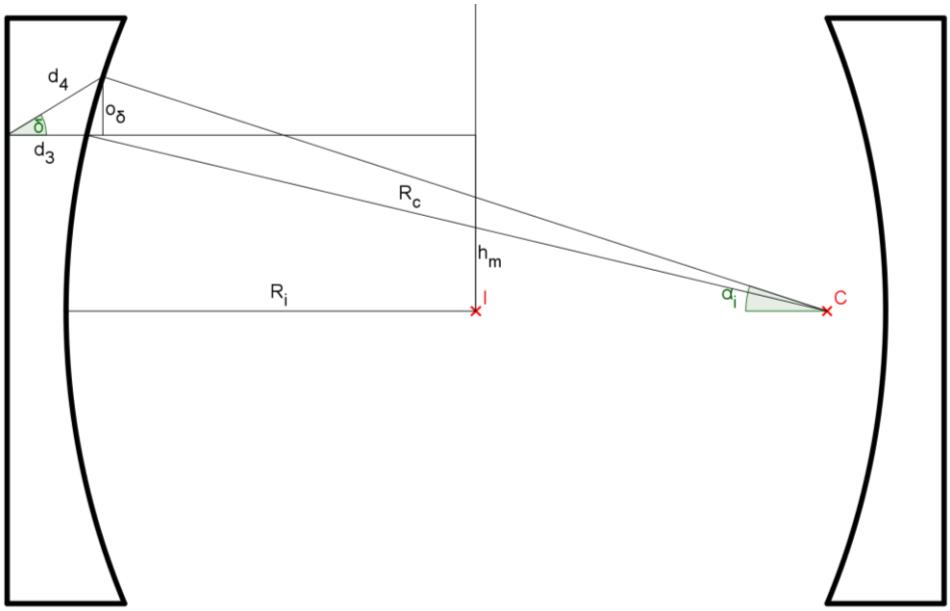

Figure 3.13: Determining thickness error from X-Axis tilt

It is necessary to distinguish between two situations here, one where the contact point on the curved surface is stationary while the other moves and one where the opposite is the case. It is obvious that the situation where the contact point on the straight surface stays stationary is always worse. The reason for this being that the cosine error resulting from the diagonal measurement is present in both cases but when the sensor moves along the circular surface it is also pushed towards the centre of the bearing. We therefor focus on this worst case.

To find the measured thickness we first determine the horizontal thickness that would be measured at the height of the sensor on the circular side d_3 via (16).

$$d_3 = R_o + R_c(1 - \cos(\alpha_i)) - R_i \tag{16}$$

Where α_i is the angle between the horizontal line and the line connecting the inner contact point with the centre of the bearing. This angle can be found via (17)

$$\alpha_i = \sin^{-1}\left(\frac{h_m + d_3 \tan(\delta)}{R_c}\right) \tag{17}$$

where δ is the tilting angle. Because this equation also contains d_3 we need to solve for d_3 which can be done with a CAS and is not shown here. The measured thickness d_4 is finally found by multiplying d_3 with the cosine of φ as shown in (18).

$$d_4 = \frac{d_3}{\cos(\delta)} \tag{18}$$

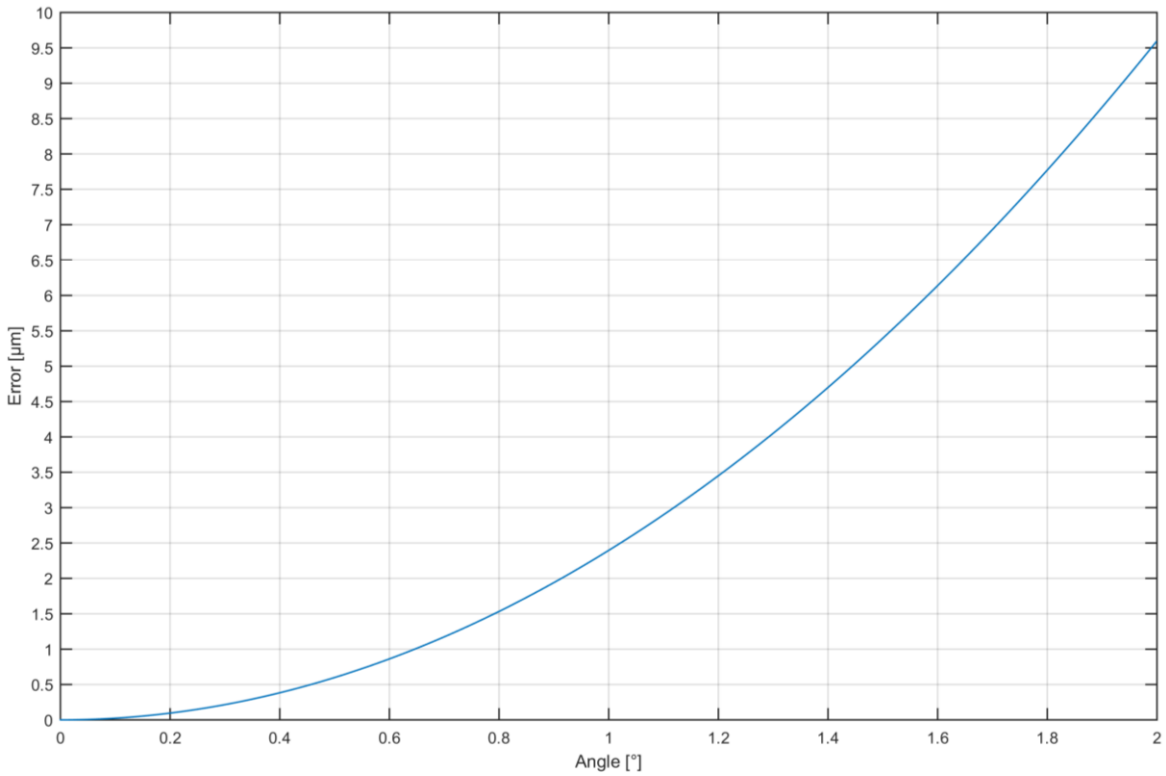

Figure 3.14: Resulting error over tilting angle (X-Axis)

The graph for this equation shown in Figure 3.14 reveals that in many cases this type of error is bigger compared to the errors resulting from the offsets we looked at before. Because of this special care has to be taken during the design of the device to prevent this kind angular misalignment.

As a result of this analysis it can be seen that the error resulting from a translational offset in the X direction is small compared to the error from the offset in the Y direction. The rotational misalignment around the X axis is more critical than that around the Y axis but they are in the same order of magnitude. The conclusion is thus that special attention needs to be paid mainly to the correct angular alignment of the measurement head.

3.1.4 Virtual Prototype

To do a more detailed evaluation of the competing concepts a computer aided design (CAD) model for the moving device concept was constructed. This model makes it possible to compare the moving bearing system for which a physical prototype already exists and the moving device system on a more equal basis. The CAD model includes all the major mechanical components of the measurement system and adjustment mechanisms. In Figure 3.15 the model is shown including a representation of the test specimen used with the previous prototype.

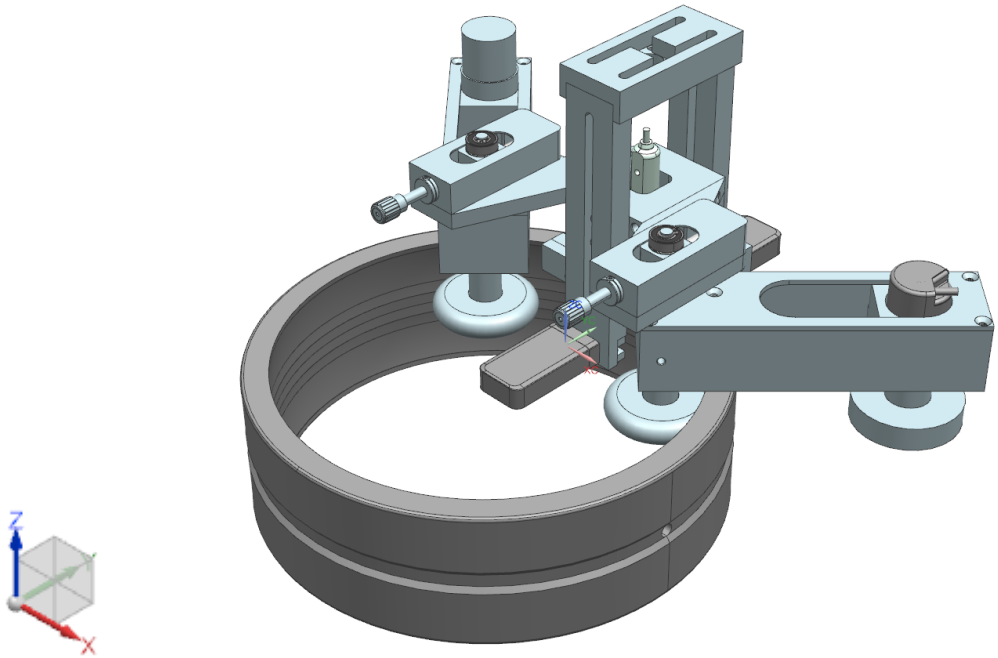

Figure 3.15: Moving device design concept

To enable a direct comparison the design needs to be able to be used on the existing test specimen but as the goal of this work is to measure large scale bearings it also needs to be able to handle bigger diameters. Although one of the benefits of the moving device concept is better scalability it became clear during the design of the model that it is not as unconstrained by the bearing size as it was anticipated.

For example the stability of the device depends largely on the width of the bearings top surface which varies with the bearing diameter. The race shape also influences the position of the contact points of the wheels that clamp the device to the bearing as well as the wheel for the rotary encoder. This can lead to further stability problems and also influence the rotation measured by the encoder. These insights are some of the results of constructing this virtual prototype. The model was also used for obtaining the values (e.g. estimated part count) necessary for the concept decision table (see 3.1.5).

3.1.5 Concept decision

To decide on the concept that should be further developed into a device design and prototype an evaluation table was used. The criteria that were considered here are aligned with the research question and focus on cost, ease of use and measurement quality. These criteria are then subdivided into more tangible categories to be evaluated. The values shown in the table are estimated by a committee based on the data gathered from the existing prototype and the virtual prototype of the alternative design. These base values were then normalized to reflect the relative difference between the concepts, weighted and then summed up. If not noted otherwise the values are given in arbitrary units relative to each other, this is possible due to the normalization mentioned before. The result which is shown in Table 3.3 is a rating between one and zero representing the overall alignment of the concept with the goal of this work. This was undertaken in order to make the decision as objective as possible.

The first category is manufacturing, specifying the effort needed to manufacture both concepts. This is represented as cost and manufacturing time because the second was also important to the realization of this project within the given timeframe. The number of parts for the moving bearing concept are estimated based on the previous prototype while not counting any parts that are either not essential to its function or which could be made obsolete in an improved design. The parts of the moving device are assessed on the basis of the virtual model (see 3.1.4).

Secondly adaptability needs to be looked at as one of the goals here is to make a device suitable for large scale bearings. Assessing the scalability is more complex than it might seem at first since there are many factors that determine if a device is usable for a certain bearing. Looking at the more conventional design the obvious limitations here are the bearing diameter and height since the device needs to be able to fit the bearing.

In case of the moving device these dimensions are not as important since the device itself can be much smaller than the bearing element. Here other factors such as the ring thickness or race curvature become relevant since the device relies on contact to the upper and side surfaces. A too narrow upper surface leads to the device sitting in an unstable position on top of the bearing.

Making the device wide enough to fit very thick rings makes it more unstable for narrow rings and also necessitates longer tactile probes if the top surface is much wider than the point at which the thickness is to be measured. In this case the curvature of the race on one side opposed to the straight surface on the other side also leads to different forces on the support bearings that the device rests upon as the surface normals are not parallel. In other words if the race is curved significantly it becomes more difficult to stabilize the device. The curvature of the race is not directly tied to the overall dimension of the bearing so the range of possible bearings can only be estimated. This was done based on looking at different bearings in the applicable size range and comparing their geometries. General bearing geometries examined here are cylindrical roller bearings, ball bearings or spherical roller bearings hence the number of supported bearing geometries.

The measurement quality was assessed based on the sensitivity analysis which revealed that especially angular misalignments lead to significant measurement errors. This is the most important reason why the instability of the moving device design leads to less precise measurement because its position relative to the bearing is not maintained by geometric constraints but by clamping forces and friction between the bearing and the supporting guide rolls (see Figure 3.15). In terms of weight and handling complexity the moving device has an advantage since it enables measurement without transferring the bearing onto the device. Because the moving device can be small than the bearing itself it can be easily stored, handled and transported.

Criteria	Type	Base Values		Norm. Values		Weight	Product	
		MB	*MD*	*MB*	*MD*		*MB*	*MD*
Manufacturing								
Number of Parts	Min	25	33	1	0,76	0,05	0,05	0,04
Part complexity	Min	1	2	1	0,50	0,06	0,06	0,03
Part size	Min	3	1	0,33	1	0,06	0,02	0,06
Cost [€]	Min	2500	5000	1	0,50	0,08	0,08	0,04
Adaptability								
Scalability Range [mm]	Max	189	760	0,25	1	0,11	0,03	0,11
Bearing Geometries	Max	3	3	1	1	0,04	0,04	0,04
Measurement Quality								
Max. parts in chain	Min	23	19	0,83	1	0,08	0,07	0,08
Trueness [µm]	Min	3	5	1	0,60	0,17	0,17	0,10
Repeatability [µm]	Min	1	3	1	0,33	0,11	0,11	0,04
Sensitivity to environment	Min	1	2	1	0,50	0,14	0,14	0,07
Usability								
Weight [kg]	Min	10	5	0,50	1	0,03	0,02	0,03
Size [m^3]	Min	0,03	0,01	0,33	1	0,04	0,01	0,04
Handling Complexity	Min	1	2	1	0,50	0,03	0,03	0,02
							Results	
						Sum	0,82	0,69
						Norm. Sum	**1**	**0,84**

Table 3.3: Concept scoring table (MB = Moving Bearing, MD = Moving Device, Norm. = Normalized)

As a result of this rating given the shown weights the conventional or moving bearing design was judged to be superior in this kind of application. Therefore the design effort described in the later chapters is focused on improving the key aspects of this design, building a new prototype based on that and evaluating its performance.

3.2 Design

In this part of the work the overall design of the device is explained and its design features and possible trade-offs are presented and justified. This relates not only to the mechanical design but also to the surrounding measurement framework composed of software and electronics.

3.2.1 Overview and goals

As the overall concept of the new device is similar to the original concept of the previous prototype the main goal here was to improve the measurement quality and ease of use by addressing the shortcomings identified and described in the previous chapters. Making the measurement process simpler and therefore faster and more precise is possible based on the initial experience gathered while testing the older prototype. Figure 3.16 shows the CAD model of the device including the measurement head and adjustment systems.

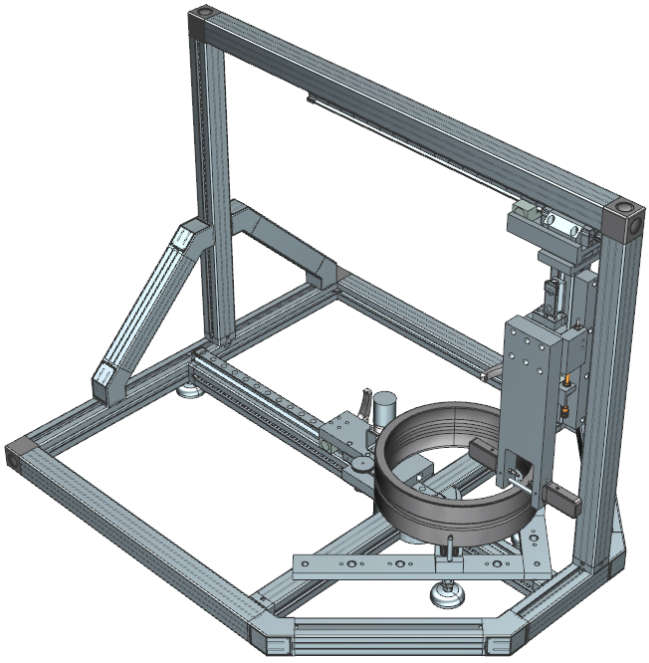

Figure 3.16: CAD model of the developed bearing element measurement device

The new device is constructed in a similar fashion to the existing prototype, namely it uses aluminium profile struts as its base frame. While the lower frame of the existing design consisted of multiple layers of struts to accomplish the 45 degree angle between it and the top cross beam the new version makes use of 45 degree connection elements, this makes it both easier to assemble the device and align the different struts to each other.

The base is no longer a full square angled at 45 degrees, only the side where this is necessary for the linear guidance of the support bearings is angled compared to the rest of the device. This enables the measurement of bearings that are bigger compared to the overall size of the device since up to a certain size only the longitudinal sides of the device have to grow to accommodate bigger bearings. Theoretically measuring such a large bearing it would then extend beyond the sides of the device.

The base structure is stiffened by cross braces tying together all the parts that carry the load exerted by the bearing. The feet carrying the device are positioned in such a way that the load is transferred between the supporting points of the bearing and the ground through the shortest path possible thereby avoiding unnecessary deformation and frame distortion.

To eliminate unwanted relative movements and misalignments the linear guidance system that was based on the profile struts itself has been replaced by profile rail linear guides namely crossed roller rail guides with low tolerances and high pretension that are recommended for measurement applications (Bosch 2014, p. 47). These also allow for the use of standard manual clamping elements which make adjustment of the device to any bearing size easier while avoiding misalignment during the clamping process.

Centring the bearing to be measured by moving all three support bearings (see p. 12) is no longer necessary as the measurement position in the X-direction can be directly adjusted through a micrometre screw connected to a linear translation stage mounted to the top cross member. Combined with a software feature to locate the minimum thickness (see 3.2.4) adjustment is less time consuming and more precise while avoiding accidental movement during the adjustment process.

A calibration rod mounting bore is incorporated into the measurement head. This rod is inserted to the head and is then set down on the bearing elements top surface. This position is then recorded with the Z-axis measurement system consisting of a magnetic linear scale connected to the same type of measurement card as the tactile sensors. The recorded position can successively be used as a reference point for the height adjustment as the position of the measurement rod in the Z direction compared to the probe tip location is known. The position in the Z direction can be roughly pre-set by hand utilizing the linear guide and a clamping element. The height is then adjusted using a fine adjustment screw connected to that clamping element. Unlike the previous prototype it is thus possible to measure the thickness at a well-defined height relative to the bearings top surface.

The measurement head consists of a single piece fork as opposed to the previous 4 piece fork. This reduces the alignment error of the sensor axes to each other to the manufacturing tolerances of the bore that they are fitted into. The layout of the measurement fork is designed in such a way that it minimizes misalignment during manufacturing by making it possible to do all the necessary material removal from the same direction. This also opens up the possibility of avoiding distortion of the fork by using wire erosion to cut out all major features.

To improve the setup process of the device it is now possible to touch the tactile probe tips against each other to zero them, avoiding the use of a calibration block. This makes a significant difference because if such a block is used it is necessary to align it so that the distance between the tips is actually equivalent to the block size and there is no cosine error. This alignment proved challenging during the initial testing of the previous device (see 2.3.1).

A trade-off between measurement quality and ease of use has to be made while deciding the dimensions of the fork. A version with longer and more separated prongs can accommodate a wider range of bearings and makes replacement of the fork between measuring those different bearings unnecessary. Because the sensor tips could then no longer be touched together either a calibration block has to be used again or sensors with a bigger measurement range have to be used. The consequences of doing the former are described above while the sensors required for the latter usually have the drawback of a lower physical resolution. In this case the solution featuring a smaller fork was chosen as using the same sensor size offers better comparability with the older device.

3.2.2 Features

The individual parts and features of the device will now be described in detail. Figure 3.17 shows the side view of the device and enumerates all the main features.

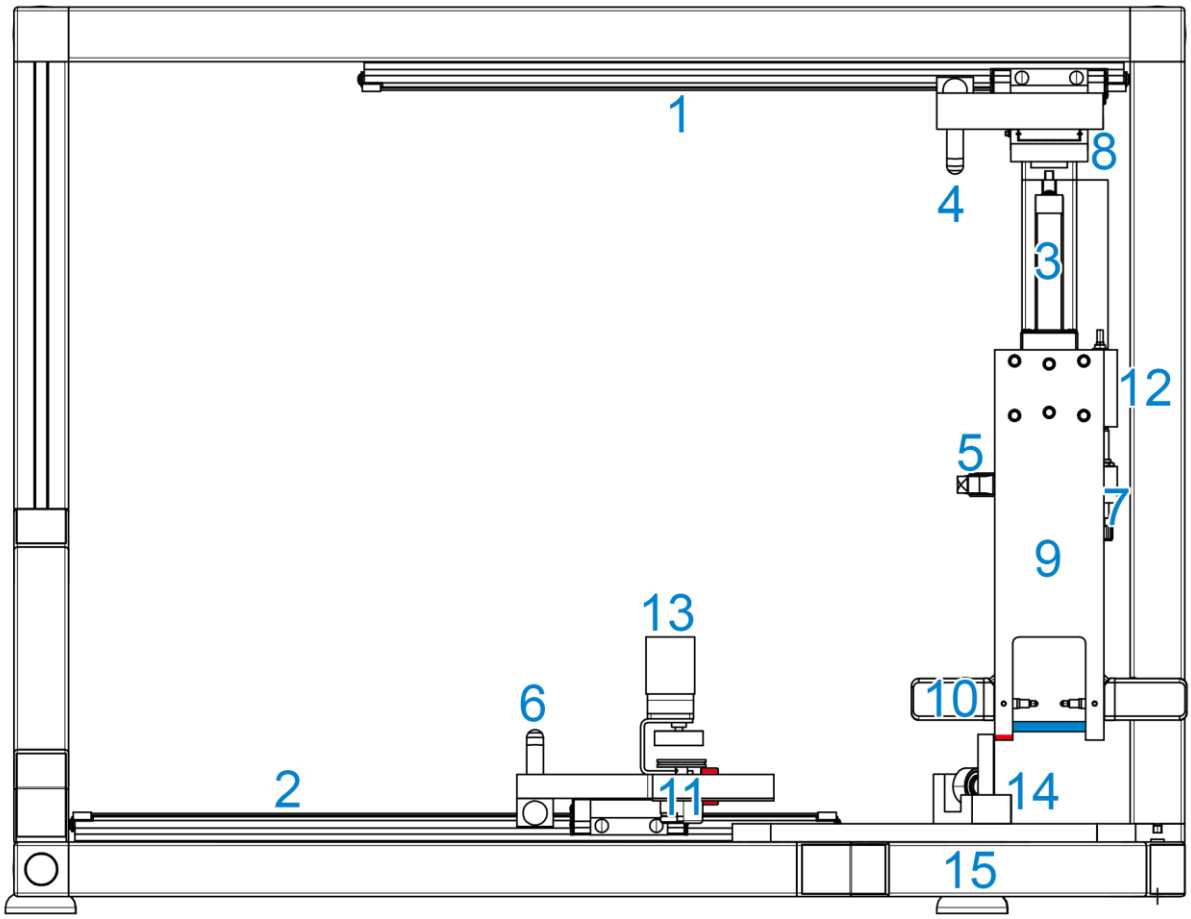

Figure 3.17: Draft of the new bearing measurement device (Side view)

All large linear movements of the device are made using the linear guides 1 (Y1), 2 (Y2) and 3 (Z). Y1 and Y2 are mainly useful for inserting the bearing to be measured into the device or fitting the device to different bearing sizes. The length of the Y2 axis is necessary to allow for these different dimensions. Although the measurement is usually taken with the Y1 axis in a position on the right side close to the one shown in Figure 3.17 the length of the Y2 axis allows for moving the measurement head over the Y1 axis, this is useful for self-alignment purposes (see 3.2.3).

Meanwhile the Z axis sets the height at which the thickness is to be measured. Because of this the Z axis is also the only axis of which the position is monitored with a sensor (12). In this case an incremental magnetic linear gauge is used which can be directly connected to the same measurement interface as the other sensors used here. This type of measurement easily allows for a large measurement range compared to systems like the tactile probes used for the thickness measurement without sacrificing too much accuracy. While the accuracy is typically lower than these other systems it is still on the order of ± 1 μm which is sufficient for the Z axis (see Figure 3.9).

The zero position for the Z axis is obtained by placing the calibration rod (shown in blue) into the measurement head and touching it to the reference surface of the bearing. The axis can then be electronically zeroed in the software (see 3.2.4). DIN 620-1 defines the reference surface as the non-inscribed surface (DIN 620-1, p. 4). In this case however as the bearing is rotated it is advisable to place the non-inscribed surface on the support bearings (14) and then zeroing the Z axis on a flat part between the lettering. This minimizes vertical movement and vibration during the measurement.

Adjusting the different axes is done by manually moving the gliders on the rails and then clamping them down using the clamping elements (4, 5, 6). In case of the Z axis the position can then be finely adjusted using the adjustment screw (7). The thread pitch of 0.254 mm per revolution used on this screw allows for very fine adjustments to be made. Setting the X axis (into the viewing plane) position is accomplished through a linear translation stage (8) with a micrometre screw attached to it.

Monitoring the rotational movement of the bearing is achieved by a rotary encoder (11) which is mounted directly to the Y2 axis carriage. To press the encoder against the side of the bearing two constant force springs are utilized. These sheet metal springs work by being unrolled from a freely rotating shaft. The internal friction and the spring force are balanced in such a way that the resulting force is constant no matter how far the spring is drawn out. In this case these springs where chosen to achieve two goals. They should keep the slippage between the bearing to be measured and the encoder wheel constant as long as the friction between the two is constant. Most importantly they guarantee that the maximum shaft load of the rotatory encoder of 10N in the radial direction (Heidenhain 2015, p. 51) is never exceeded.

The sensors used in this device are fitted to the fork using a reamed fitting hole and a perpendicular grub screw. Compared to the clamping mechanism of the previous device this leads to less change in the position of the sensors while affixing them to the fork. Since the set screws are perpendicular to the Z axis no noticeable movement in the Z direction should occur which is important as the distance between the calibration rod and the sensors in this direction has to be known to obtain the sensing height.

The feet of the device (15) are adjustable in height and conform to the angle of the ground the device is resting upon. They also feature some dampening to prevent vibration being transferred into the device. For larger bearings the feet can be moved from the outer frame of the device to the support bearing holders themselves. By placing the feet directly under the bearing the frame deformation is minimized. This however only makes sense if the bearing to be measured is heavier than the device frame itself as in this case the guide rails have to support the frame instead of the bearing.

The support bearings (14) are attached to machined and ground guide rails. They are positioned using locating pins and then bolted down. Because two pins are needed to position them but the distance between the two corresponding holes on both the guide rail and the support bearing holder can be slightly different the holders cannot easily be removed from the guide rails after fitting them. To prevent this problem threading for a push-out screw was incorporated into the holder. This allows for easy removal by inserting a bolt and pushing the holder up from the rail using the bolt force. During measurement the bearing to be measured rests against two steel shafts with smaller support bearings. These shafts extend upwards from the support bearing holders. As these surfaces do not carry the weight of the bearing the normal force that they are subjected to is minimal.

3.2.3 Self-alignment procedure

The device is designed to aid in the alignment of the long linear guides (1 and 2) to each other. To accomplish this the Z axis magnetic linear gauge can be used to measure the distance between those two guides at different points. This way the parallelism of these rails along their direction of travel can be checked.

The edge of the sensor head (shown in red in Figure 3.17) is set down onto the support bearing (also shown in red) on the drive sled. Following that the Z axis value is zeroed in the bearing measurement software. The measurement fork as well as the drive sled are then moved in unison along their corresponding linear guides and the Z axis movement is monitored. Although it is not possible to determine the absolute distance between the two rails this way measuring the variation is enough to evaluate and adjust the alignment.

Using the built in Z axis measurement system eliminates the need for additional measurement devices and ensures that the measured parallelism is taken in the same frame of reference as the actual bearing element measurements.

3.2.4 Software

For every measurement device the whole system has to be taken into account when trying to achieve results that are as close to the true value as possible. This also includes the software that should make the measurement process quicker while also enhancing the accuracy and preventing user error. For this purpose a custom tool was developed in C# which helps the operator to set up and calibrate the device. The initial setup is assisted by a display that shows if the probes are currently close to the minimum value that has been detected since starting the software. This value can also be reset in case the software has been started before a bearing was placed into the machine or something was changed in-between.

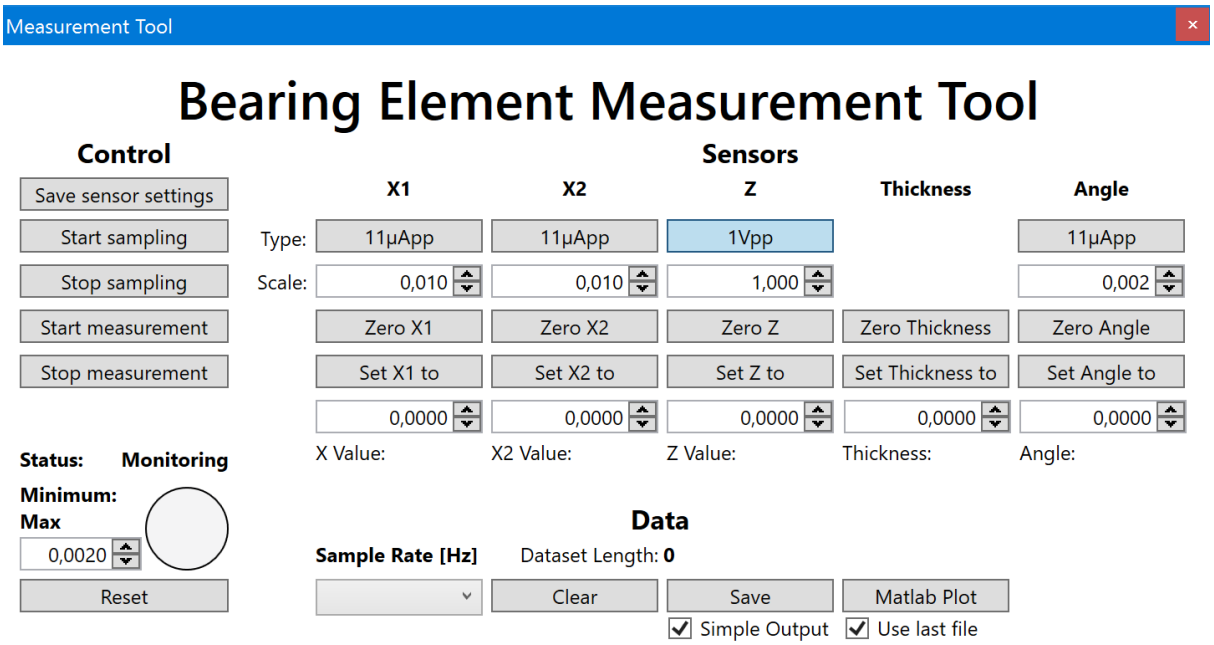

Figure 3.18: Graphical user interface of the developed measurement software

The minimum display is sized appropriately so that the operator can look at it from a distance while adjusting the device. The width of the range that the software classifies as close enough to the minimum can be selected freely. Utilizing this capability the calibration can be done in iterative steps from rough to fine which helps speed up the process.

The measurement head for the test specimen that was used is designed in such a way that the sensor probes can touch each other so that the measured value can be zeroed and no length artefact is necessary for calibration. However for different sensor fork geometries the software also includes the possibility to calibrate the individual sensors including the Z axis gauge as well as the computed thickness to any value.

The data can be recorded at sampling rates up to 5kHz with 32bit resolution and 12bit interpolation (Heidenhain 2011, p. 71). Interpolation is done in hardware by the used data acquisition cards.

The resulting data is stored as a comma separated values file. Two different formats are supported. The user can choose to either just store the measured thickness and the associated rotary encoder values, which is usually sufficient for analysis, or he can alternatively choose to store the individual sensor values as well, which is useful mainly for debugging purposes. For ease of use and quick examination of the measurement results and quality the data can automatically be transferred to Matlab where a script included with the software subsequently supports plotting and analysing the data.

3.3 Analysis Methodology

As with most measurement systems that involve sensors, measuring something is only the first step of obtaining the actual data or measurement that is sought. In this case after the data is captured using the developed device and software it is processed by a series of Matlab scripts. The function of these is detailed below.

Because the sensor signals are captured in the time domain using the hardware clock of the interface cards the data is not necessarily sampled at equally spaced angles around the bearing. To correct this the rotary encoder data is utilized to resample the thickness at equally distributed positions, this is sometimes also called adaptive resampling (Blough 2006, p. 2). Linear interpolation was used to approximate the angle based signal. Bechhoefer et al. have shown for an application that is comparable to the one described here that this type of interpolation does not perform worse than for example spline based interpolation (Bechhoefer, Kingsley 2009, p. 4). Oversampling is used to minimize any aliasing or other negative effects during this resampling.

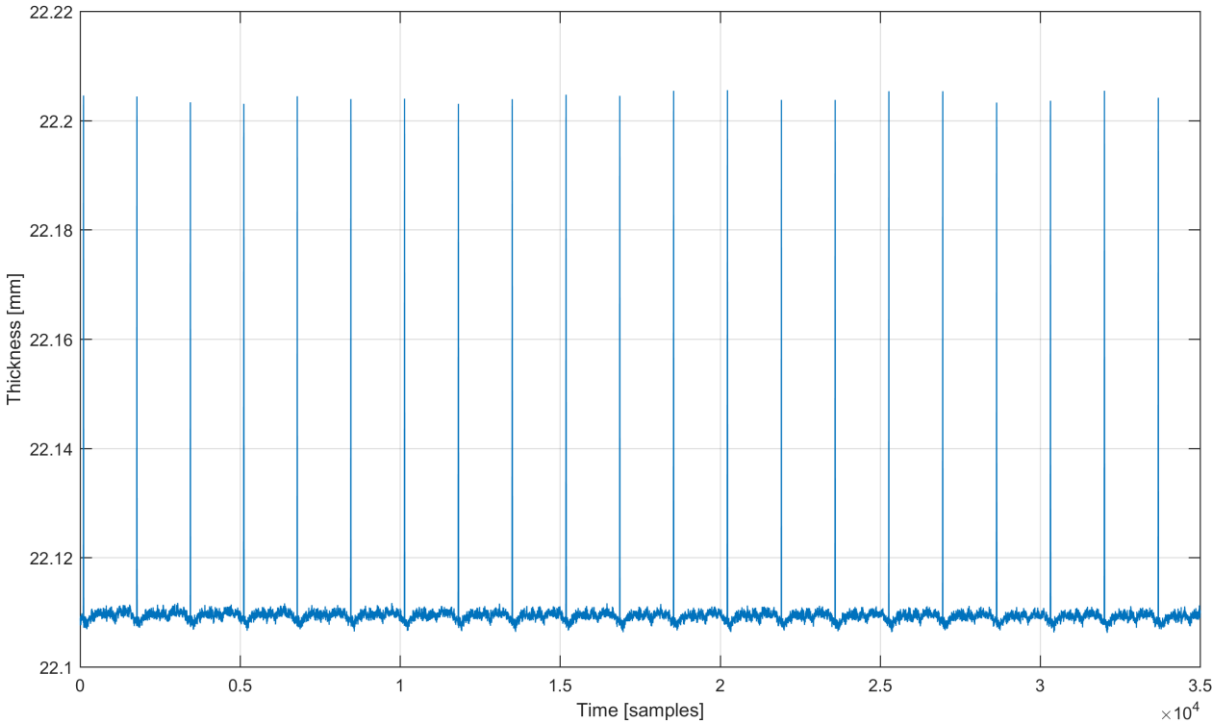

Figure 3.19: Raw thickness data for multiple rounds

The next step of data processing is segmenting the long continuous dataset that entails multiple measured rounds (see Figure 3.19) into the individual rounds. Doing this in software instead of using a dedicated hardware trigger that signals the beginning of every round has advantages and disadvantages. An advantage would be that there is no need for an additional sensor and input channel (or in this case whole additional interface card) which lowers complexity and cost of the device. The negative side is that additional software has to be developed to recognize the beginning of a new round. Depending on how this is done it leads to a less precise matching of the measurement data across the individual rounds.

For the prototype made as part of this work a software implementation based on recognizing a small tape marker placed on the bearing to be measured was chosen. This marker increases the apparent thickness of the bearing in a specific position, this jump in thickness (shown in Figure 3.19) can later be recognized by the software. Because of the width of the marker a segment of the thickness data roughly equivalent to half a degree of the bearing cannot be used. This of course depends on the bearing diameter and can be improved by using a smaller marker and if necessary a higher sampling rate.

The developed program first searches for peaks within the overall data. It then checks for rising and falling edges close to these peaks. The end of the falling edge marks the beginning of a new round while the start of the rising edge indicates the end of the round. The data between those flanks is the unusable tape section mentioned before. Because of the tape and sensor head geometry the observed flanks have been around 2 samples in duration at 100Hz sampling rate, this equates to an angular positioning accuracy of around half a degree at the used bearing diameter and rotational speed.

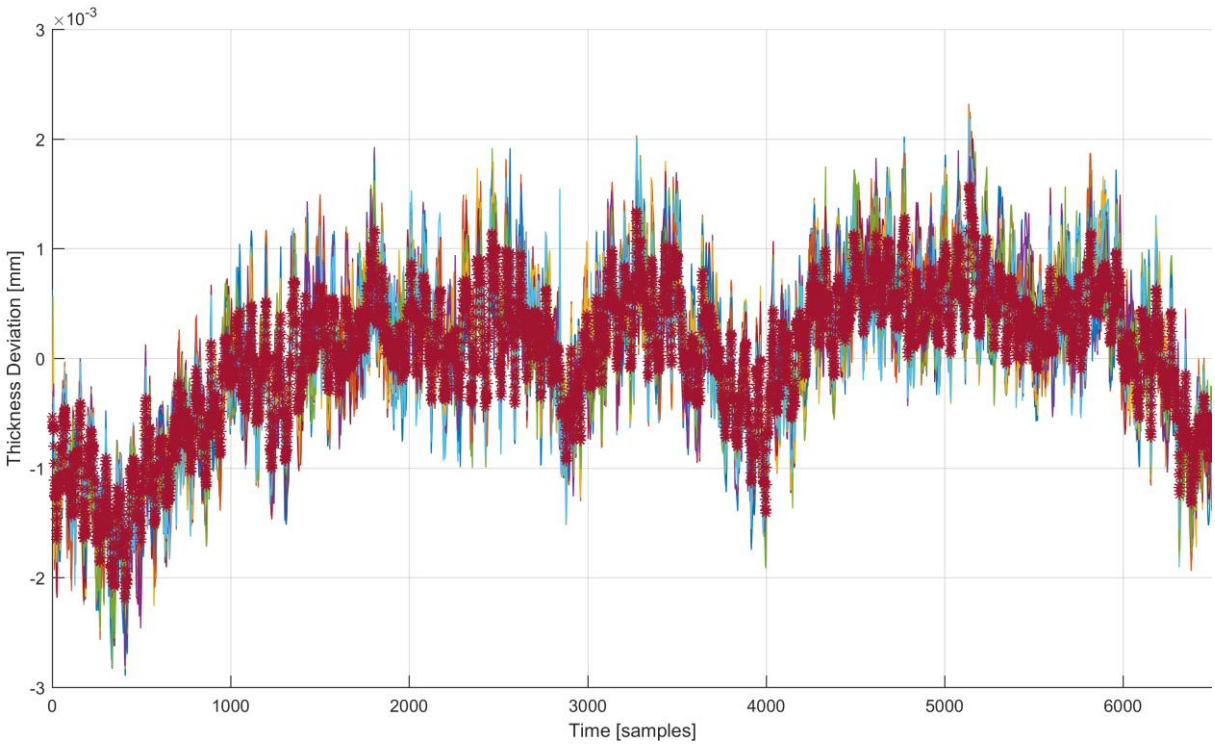

Figure 3.20: Raw and averaged thickness variation (20 rounds)

After this step of processing is completed the individual data segments need to be processed further. Figure 3.20 shows the raw data from 20 segments respectively rounds as well as the resulting average (marked dark red). To remove random noise and error from the data a number of rounds are summed up and averaged.

The effect of this step depends on the number of rounds that are averaged, the precision of the alignment between rounds and the actual averaging process used. Averaging can be done in the time domain or in the frequency domain. Averaging in the frequency or modal domain works by first applying the Fourier transformation, than averaging and then doing the inverse transformation. Averaging in the time domain can be problematic because of the angular positioning accuracy. Simply described it might not always be the case that high and low peaks cancel each other out because their angular position is slightly shifted. For a high enough number of rounds and good enough angular accuracy this should not be a significant problem. Figure 3.21 shows a comparison between both methods. There is a slight difference at the edges which likely is the result of the implicit assumption of periodicity during the Fourier transformation which is not strictly true due to the missing portion where the marker is placed. Overall both averaging methods match within 0.1 μm. Time domain averaging was used for all datasets presented in this report if not otherwise noted.

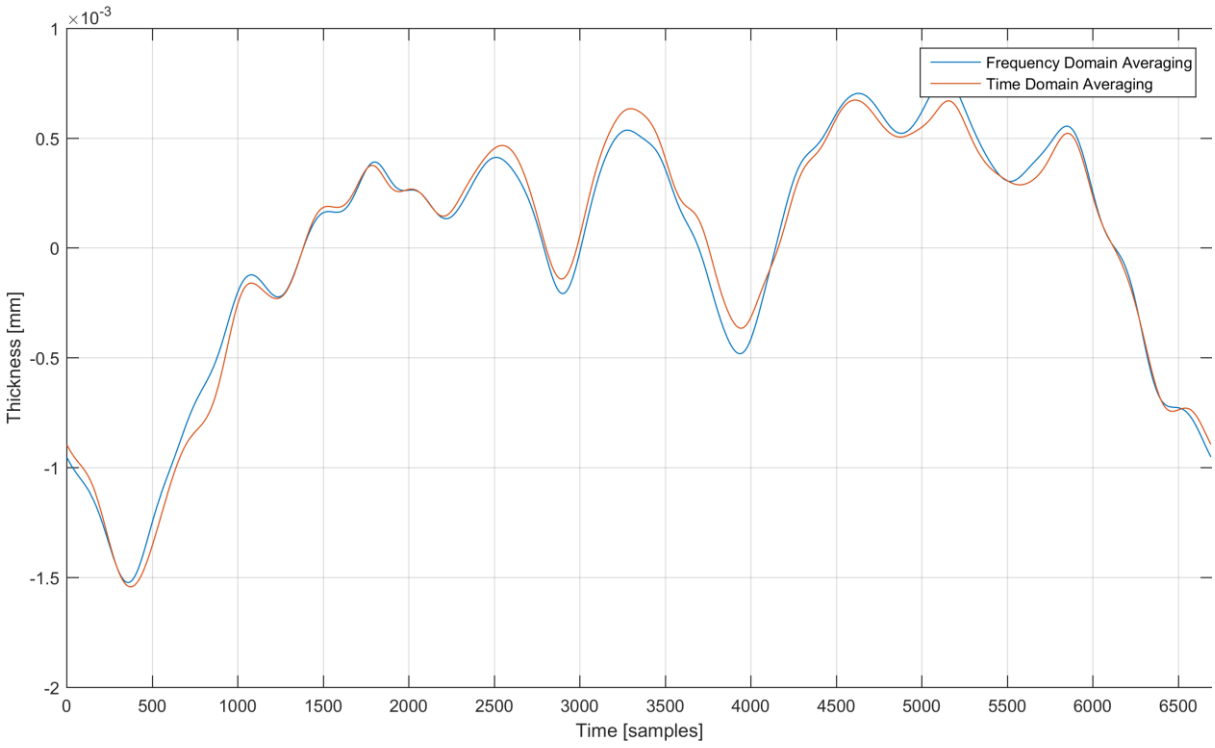

Figure 3.21: 20 rounds averaged in the frequency domain and in the time domain

The averaging process results in the data being combined into a single record representing the apparent thickness at equally spaced angles around the bearing. This record still contains some amount of random noise and error as well as surface roughness features. Because all of these are unwanted here filtering is necessary.

A low pass filter is employed to remove the undesired frequencies. DIN EN ISO 16610-21 specifies a Gaussian filter for use in geometric product specification applications and specifically for closed profiles (DIN EN ISO 16610-21, p. 11). While the frequency response of this filter is equivalent to a conventional low pass filter the benefit of this filter is its linear phase response.

This is also called phase correct or phase neutral and overall only leads to a delay of the signal as a whole but does not influence the position of peaks relative to each other. As a downside this filter cannot be implemented using a traditional resistor capacitor network. It also cannot be used in live, latency critical applications as it is non causal or in other words needs to know how the signal will look at a later point in time to determine the amplitude of the filtered signal at the current point in time. Because it is only used for digitally post processing the already captured data here these downsides do not apply.

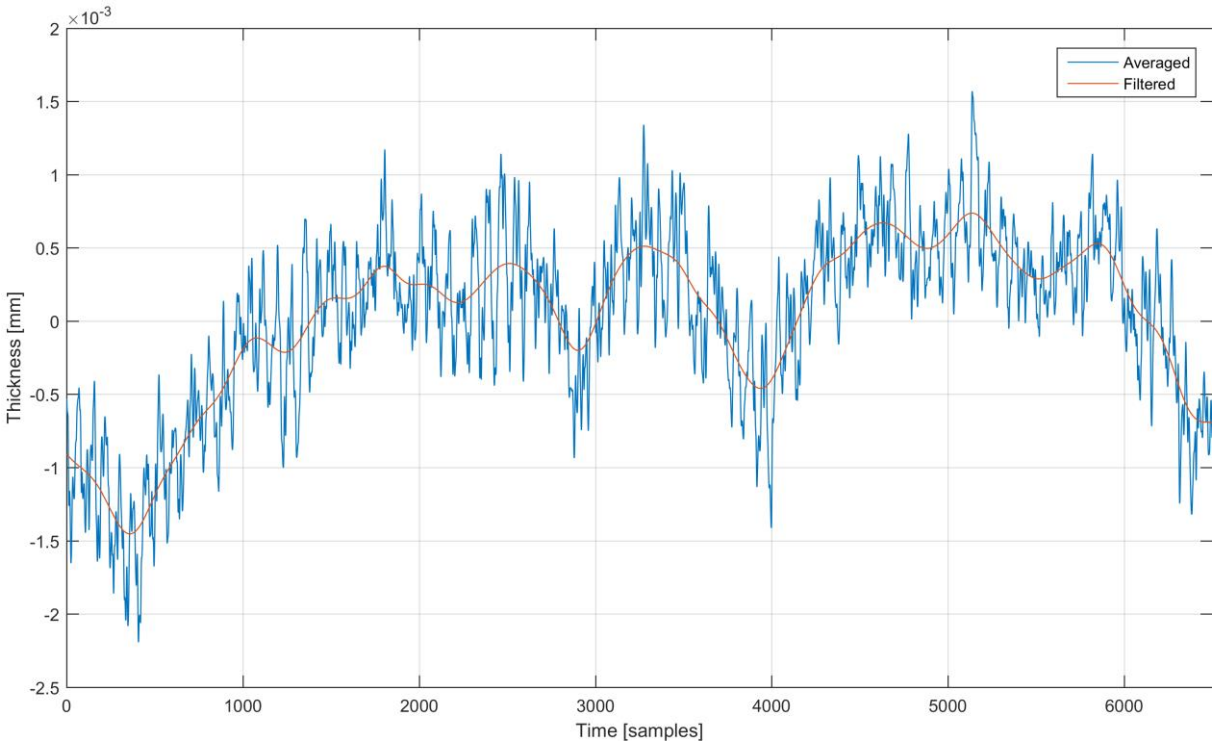

Figure 3.22: Thickness deviation averaged over 20 rounds and filtered with 15 UPR

The filter is implemented by first generating a Gaussian kernel whose width is determined by the original sampling rate and the desired cut off frequency. This kernel is then applied to the signal using circular convolution. Applying a Gaussian filter can be problematic as it usually needs an input signal length that is longer than the examined section (Hernla 2000, p. 129). Circular convolution avoids this as it interprets the signal as periodic (Muralikrishnan, Raja 2009, p. 19). The filter averages out the possible difference between the start and end of the signal which might be present because of the part of the ring that is missing due to the marker strip or measurement error, this is acceptable as long as the strip is sufficiently narrow. The measurement results described in this report are generally filtered with a cut of frequency of 15 undulations per rotation (UPR) if not otherwise noted. Figure 3.22 shows the signal after the averaging described before and finally after the filtering.

3.4 Testing and validation

To evaluate the overall measurement quality of the prototype an outer bearing element was measured using a Mitutoyo Legex 9106 coordinate measurement machine. Measurement was carried out by the national metrology institute of Finland MIKES.

Figure 3.23 shows the bearing element during measurement at MIKES. The CMM has a quoted length measurement error of 0.3 μm + L/1000 μm where L is the measured length in millimetres (Mitutoyo 2014a, p. 2). This equates to 0.72 μm for the largest dimension of the bearing used here (420 mm diameter).

The bearing features a ground cylindrical surface as well as a spherical race originally meant for the spherical bearing elements. This geometry allows for testing the measurement device in two slightly different applications while only having to measure a single part. This is especially useful as the measurement process on the CMM takes several hours but can determine the thickness at different Z positions without additional time being spent.

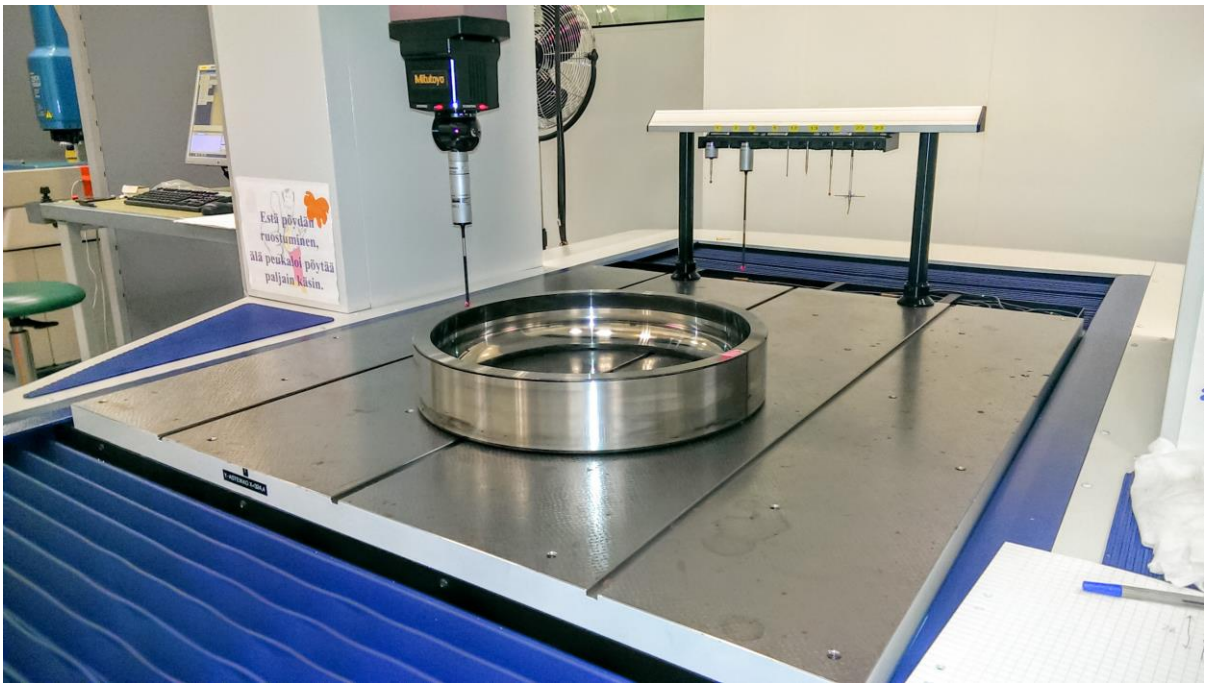

Figure 3.23: Bearing element during CMM measurement

This is because of the way the CMM was programmed to measure the bearing element. It first scans a line along the Z direction on both the inside and outside of the ring. The distance between those two lines at different Z positions can then be calculated. This way the influence of the probe diameter on the measurement result can be minimized. Otherwise the Z position of the point where the spherical stylus tip touches the spherical bearing race would not be the correct Z position. The coordinate system in which the measurement is taken is aligned corresponding to the top surface of the bearing.

After the measurement was done the CMM program that was made by MIKES saved the calculated thickness for both cylindrical (Z=28 mm) and the spherical (Z=43 mm) surface to a file. This file was then further processed using the same Matlab scripts that are used for analysing the results from the thickness measurement machine prototype (TMM).

To look at the repeatability of the TMM both surfaces where measured using it 20 times with 20 rounds each. Between every measurement the machine and software was completely reset and zeroed using the calibration rod and by touching the sensor tips against each other. This was done to simulate the repeatability for real world measurement applications.

Another set of scripts was made to process this dataset. The filtered as well as the unfiltered data is used to generate comparative results such as the maximum difference between the measurements as well as statistical values such as the distribution of the mean thickness. The data from the coordinate measurement machine is then used to compare the measurement quality against this reference instrument. Here the differences are looked at both in terms of thickness variation as well as absolute thickness. The results of this analysis are described in the following chapter.

4 Results

This chapter will initially focus on the results obtained using the new prototype and their repeatability. Thereafter the agreement with the CMM measurement will be looked at and the reasons for potential disagreements will be discussed. For the first part the focus will lie on thickness variation measurement quality. While this is the more important parameter for the second part absolute accuracy compared to the reference will also be looked at.

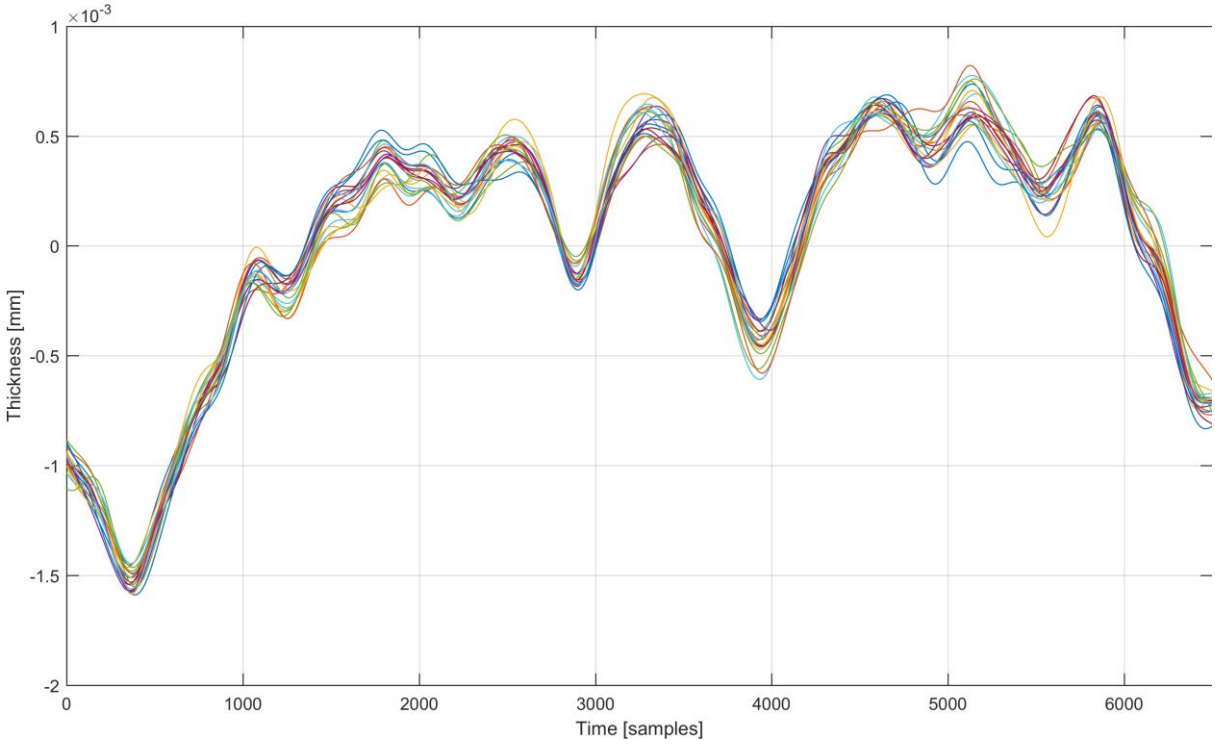

Figure 4.1: Filtered data from cylindrical surface compared over 20 rounds

Figure 4.1 shows the measurement results for 20 measurements calculated from the average of 20 rounds each. The individual measurements match up well and the spread is around 0.3 μm at its widest point around the 5000 samples mark. This is a significant improvement over the previous machine which only achieved around 1 μm in similar terms (see Figure 2.9).

By calculating an average thickness variation curve from the curves shown above the distribution around this mean can be analysed. In the absence of a known true value the mean can be taken as the best available substitute (Dubbel et al. 2014, W 1.4.1). The uncertainty is calculated using equation (1). For the cylindrical part the standard deviation is 9.45e-05 mm and the corresponding standard uncertainty is 2.11e-05 mm. The values for the spherical surface are slightly higher than that which is most likely due to the influence of the height adjustment error on this result. Here the standard deviation is 1.36e-4 mm while the standard uncertainty is 3.04e-5 mm. For every data point measured under these same conditions the mean value of a series of measurements made with this machine can therefore be expected to lie within a range of 4.23e-5 mm (cylindrical) respectively 6.08e-5 mm (spherical) with 95% probability (coverage factor k=2).

The distribution of the results can further be looked at by plotting a probability distribution of the mean thickness values. Figure 4.2 shows the histogram as well as a fitted normal distribution function.

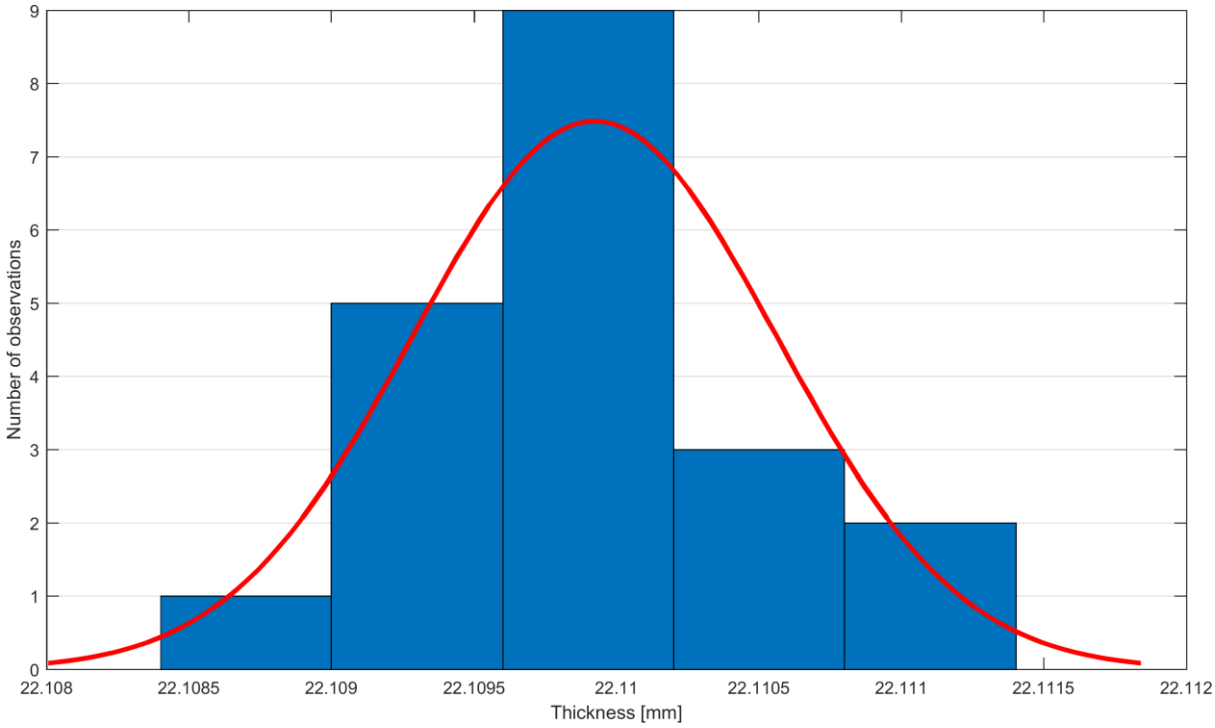

Figure 4.2: Distribution of mean thickness

Using a histogram like this can be misleading for judging if the values are normally distributed or not because the number of bins used (5 in this case) greatly influence if the plot looks like a normal distribution. There is however a statistical test which objectively evaluates the probability that the obtained values are sampled from a normal distribution. The Shapiro Wilk test confirms on the 95% confidence level ($\alpha=0.05$) that both the results from the cylindrical as well as from the spherical surface are likely to have been sampled from a normally distributed source.

While looking at the repeatability and distribution of the results provides some insight as to if this concept and prototype is suitable for measuring thickness variation it is also necessary to compare it to a known reference. Otherwise the results may be repeatable but meaningless because they lack trueness (see 2.1).

Figure 4.3 shows the filtered and unfiltered (background) results from the CMM as well as from the thickness measurement device for the cylindrical surface. There is a good agreement between both measurements around the whole circumference. At the 225 degree mark the raw CMM data includes a peak that has been truncated in the graph in favour of better representing the rest of the data. This peak is likely an outlier in the CMM data and leads to a mismatch between the filtered graphs around the same area. Overall both measurements agree within 0.3 μm whether this peak is included or not.

Comparing the difference between the mean of all 400 rounds that were measured and the reference data it can be ascertained that increasing the number of averaged rounds above 20 does not significantly improve the measurement quality.

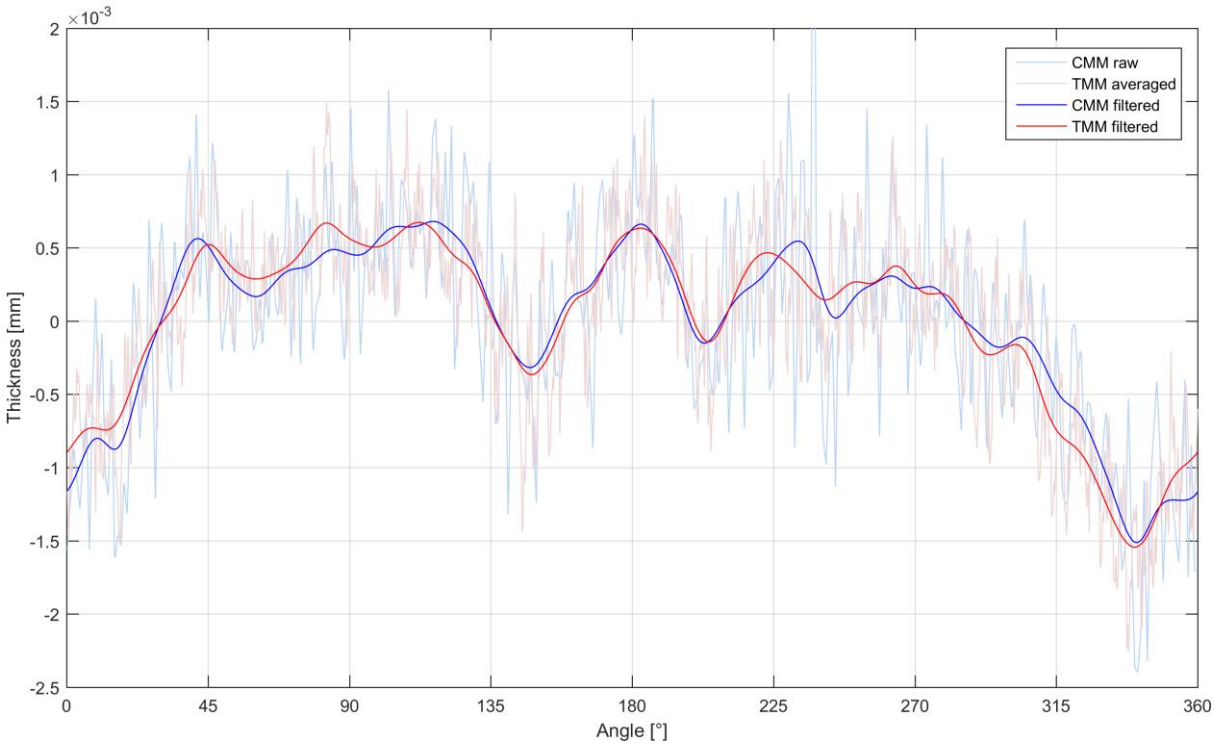

Figure 4.3: CMM vs. TMM thickness variation comparison (Z=28 mm)

For the spherical surface the measurements taken from the CMM showed a large disagreement to the TMM results. Initially it was assumed that the reason for this is that the CMM uses the top surface of the bearing as the reference for the coordinate system while the TMM does not do any coordinate transformation and therefore uses the surface that is resting on the support bearings as the reference.

To evaluate if this is the cause of the disagreement the bearing was measured again on the TMM while being turned upside down. The results of this measurement can be seen in Figure 4.4. There is a difference between the measurements taken with different bearing orientations on the same machine however both do not match the CMM result. In the polar plot (also shown in Figure 4.4) of this graph it becomes evident that there is an angular dependent offset in the CMM data. This one sided thickness difference does not fit with the manufacturing process of a bearing which consists of turning and grinding among other steps and should produce periodical waviness or similar artefacts instead.

To investigate this further the bearing element was measured again on the coordinate measurement machine. To more closely replicate the measurement process of the TMM instead of resting the bearing element on the measurement table a three point support system was used.

The CMM program was modified to use a Z reference that moves along the ring following the location at which the thickness is measured. This resulted in the elimination of the previously seen offset and in a much closer agreement between the results from the two machines. The maximum difference between the thickness variation measured by the CMM and TMM after this change was implemented is 0.7 μm.

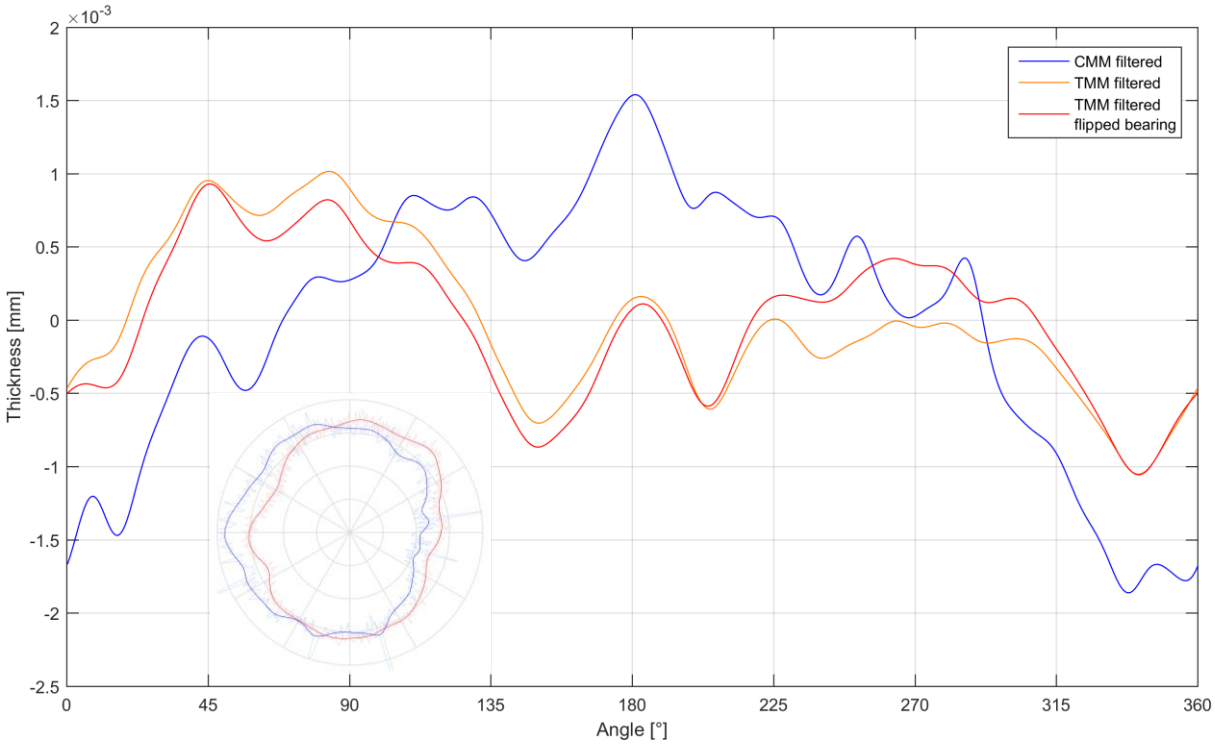

Figure 4.4: CMM vs. TMM thickness variation disagreement (Z=43 mm)

The CMM data also allows for examining the distribution of the measurement results around this reference measurement. To achieve this the CMM measurement is taken to be the best available estimate for the true value of the measurand (see 2.1).

The standard deviation around this value for the cylindrical surface is 2.62e-4 mm which equates to a standard uncertainty of 5.85e-5 mm. For the spherical surface the standard deviation around the result from corrected measurement is 6.73e-4 mm while the corresponding standard uncertainty is 1.51e-4 mm.

For the absolute thickness accuracy the mean values of 20 measurements from thickness measurement machine were compared to the corresponding CMM results. The maximum absolute difference between those two measurements is 3.5 μm for the cylindrical surface and 10.2 μm for the spherical surface. As before this difference is most likely due to the effect of Z axis positioning inaccuracy.

Figure 4.5 again visualizes the close agreement between both measurement devices in polar plots for the 28 mm (cylindrical) and 43 mm (spherical) Z position. The radial axis shows the thickness variation in μm where 6 μm was added to the mean to help with the visual representation.

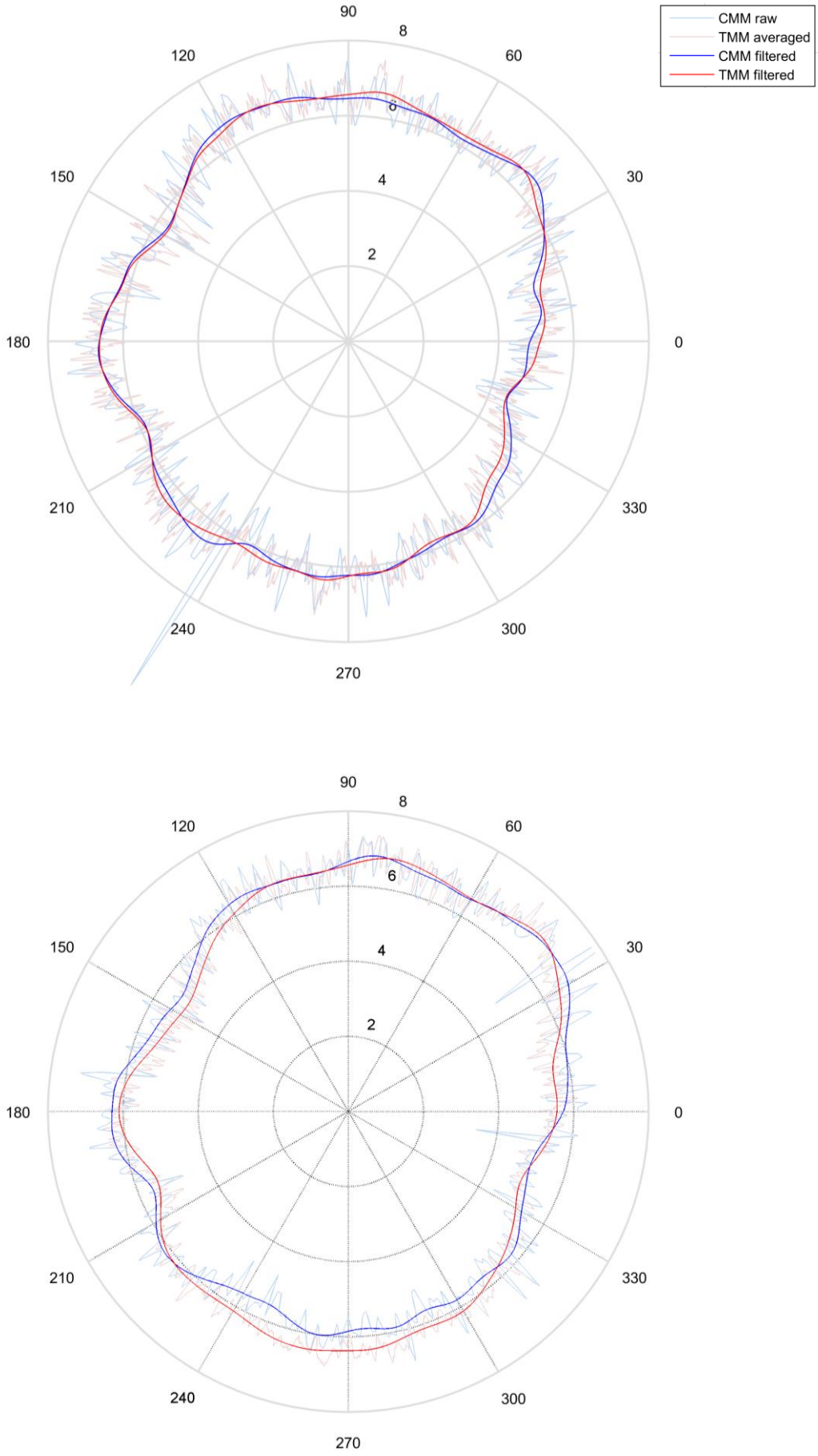

Figure 4.5: CMM vs. TMM thickness variation comparison polar plot (Top: Cylindrical, Bottom: Spherical)

5 Discussion

To determine if the prototype that was designed and manufactured as part of this work meets the implicit criteria outlined by the research question:

> Can a dedicated measurement device for ascertaining the thickness of large scale bearing elements be made in a way that it improves performance in terms of measurement quality, cost and/or ease of use when compared to existing devices in the same application?

stated in chapter 1.2 we first need to separate these criteria. The prototype should improve one or more of the following:

- Measurement quality
- Cost
- Ease of use

In terms of ease of use the prototype outperforms both the previous design as well as the CMM. In comparison with the previous machine this is mostly due to better adjustability achieved by using dedicated adjustment screws for both the Z axis and for centring the measurement head. The centring adjustment however displays a slight issue that decreases repeatability which was found during testing. Insufficient stiffness of the used linear translation stage leads to small unintentional movements of the measurement head. This could be alleviated in an improved design using a different translation stage.

Despite this shortcoming the overall measurement system still performs better than the previous version and is easier to operate. All adjustment tasks are assisted via the developed software and based on the sensors that are also used in the measurement process itself. This makes the adjustment quicker, less reliant on additional equipment and less prone to operator error.

In contrast to a coordinate measurement machine the prototype does not need to be reprogrammed for each bearing that is to be measured. Because it is a single purpose machine its operation is less versatile but also simpler than that of a CMM. This also affects the time it takes for a measurement to be taken. While the measurement process that was implemented to obtain the CMM data described in the previous chapter took over 5 hours comparable results are delivered by the TMM in less than 20 minutes including setup and alignment.

In terms of cost a quantitative comparison between the two devices is difficult as the used CMM is a commercial product while the developed device is only a prototype. The CMM also features a much larger measurement range in which it can operate. However because the prototype is a single purpose device, employing a much simpler design and using less components it generally has a cost advantage. The differential measurement principle helps reducing cost by simplifying the machine design but also by lowering the requirement on the measurement environment. Because the size of the measurement fork is small and the sensor tips can be touched together to be zeroed tight temperature control is less necessary than with a large scale CMM.

Measurement quality has been described in quantitative terms in chapter 4, qualitatively it is important to determine if the measurement results from the prototype are usable for practical applications. The absolute thickness measurement accuracy is between 3 and 7 μm depending on the surface geometry, this is an order of magnitude worse than the CMM's quoted length measurement error. Based on this the prototype cannot compete with a conventional measurement machine in this regard. For practical bearing measurement applications however the thickness variation is the more interesting quantity as it directly influences the dynamic behaviour of the assembled bearing unit. As shown previously the TMM results for this are very much comparable to the CMM results and therefore the prototype can be a good substitute for such a machine in this specific application.

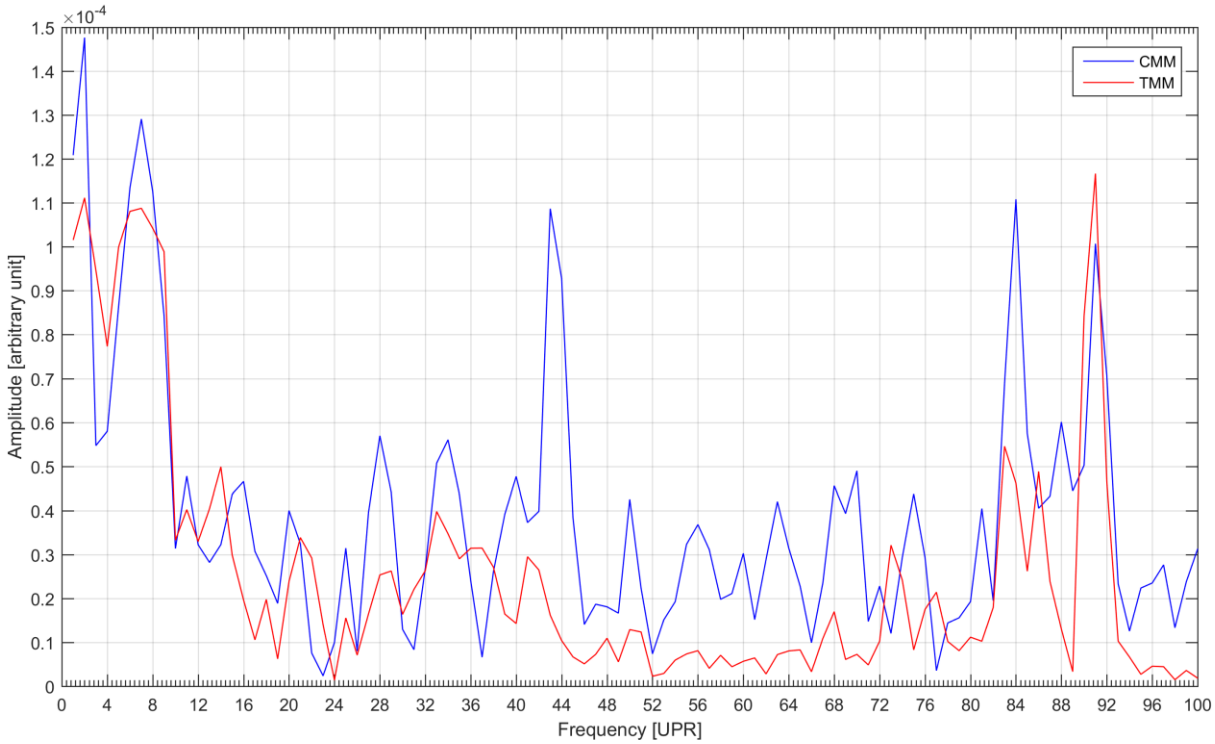

Figure 5.1: FFT Frequency spectrum comparison

To evaluate the dynamic behaviour of rotating systems modal spectra are commonly used. Figure 5.1 shows an exemplary spectrum generated via FFT from the unfiltered but averaged TMM and raw CMM data. It can be observed that the peaks at some frequencies match quite closely. However the smaller peaks between 45 and 70 UPR are much more apparent in the CMM measurement. This is most likely due to the averaging process employed by the developed measurement system helping in reducing noise and thereby isolating the actual modes of the bearing element (see also Rahman et al. 2011, p. 37).

Synchronous averaging has been used to look at bearing vibrations before (see Braun, Datner 1979, p. 120) but because here the signal of an individual component of the bearing assembly is available its application is simpler. The reason for this is that all bearing element dependent signal components repeat once per rotation in this case as there are no rollers or other elements present that would affect the measurement.

6 Summary and Outlook

This work evaluated the feasibility of substituting a commercial multipurpose measurement machine with a specialized system designed for the single task of measuring bearing element thickness. To do this a concept was made and a device was designed, built and tested. The results that are comparable to those from a conventional machine show that such a design can be viable from both an economical and a technical point of view.

In general the thickness measurement machine prototype performs well within the set application boundaries and can match or beat the performance of a conventional machine here. Outside of this scope the machine cannot compete with a general purpose machine but further iterations could enable it to do so in some aspects (e.g. absolute thickness measurement).

As part of this project a secondary concept with a moving measurement device was also looked at. This design was not realized here because it did not align with the goals and time frame of this project to the same degree as the stationary design. However this concept could still be useful for other applications and especially on very large scale bearings. There its advantages could outweigh its disadvantages because unlike a stationary device its size does not necessarily need to change with the bearing diameter. Building such a device poses significant technical challenges that would need further research to be overcome.

Further research is also warranted to increase the performance of the prototype presented here in terms of absolute accuracy, scalability and adaptability. In these areas a trade-off was made to improve the measurement quality and handling while measuring bearing element thickness variation as this was the main goal of this work. It could be possible to improve the properties that were not focused on here without degrading the demonstrated performance.

The machine described here enables fast and simple measurement of inner and outer bearing components. This capability can now be utilized to further study the influence of thickness variation on the dynamic behaviour of bearings. It can also be employed to measure the wear properties of bearing elements throughout their life time. As the device is low cost, simple to handle and has low requirements on the measurement environment it could in the future also be used outside of research applications to evaluate the condition of bearings in the field.

References

DIN ISO 5725-1:1994, 11.1997: Accuracy (trueness and precision) of measurement methods and results - Part 1: General principles and definitions, checked on 12/27/2015.

Bechhoefer, Eric; Kingsley, Michael (2009): A Review of Time Synchronous Average Algorithms. In : ACPHMS. Annual Conference of the Prognostics and Health Management Society.

Blough, Jason R (2006): Adaptive resampling-transforming from the time to the angle domain. In : IMAC-XXIV: Conference & Exposition on Structural Dynamics.

Bosch Rexroth AG (Bosch) (2014): Roller Rail Sysstems Catalog. Available online at https://md.boschrexroth.com/modules/BRMV2PDFDownload-internet.dll/R999000354_2014-05_EN_RSHP_Media_1.pdf?db=brmv2&lvid=1179795&mvid=11901&clid=1&sid=5479FD1C25ABFC791C968B9400E0D764.borex-tc2&sch=M&id=11901,1,1179795, checked on 1/19/2016.

Braun, S.; Datner, B. (1979): Analysis of Roller/Ball Bearing Vibrations. In *Journal of Mechanical Design* 101 (1), p. 118. DOI: 10.1115/1.3454009.

Dr. Johannes Heidenhain GmbH (Heidenhain) (2011): IK 220. Manual. Traunreut. Available online at http://content.heidenhain.de/filebase/files/9355/ik220_de-en.pdf, checked on 11/20/2015.

Dr. Johannes Heidenhain GmbH (Heidenhain) (2013): Metro MT 12. Data sheet. Traunreut. Available online at http://www.heidenhain.de/de_DE/php/dokumentation-und-information/prospekte/popup/media/media/file/view/file-0825/file.pdf, checked on 9/1/2015.

Dr. Johannes Heidenhain GmbH (Heidenhain) (2015): Rotary Encoders. Catalog. Traunreut. Available online at http://www.heidenhain.de/de_EN/php/documentation-information/brochures/popup/media/media/file/view/file-0034/file.pdf#page=54, checked on 1/22/2016.

Drosg, Manfred (2009): Dealing with Uncertainties. A Guide to Error Analysis. 2nd, enl. ed. Berlin, Heidelberg: Springer-Verlag Berlin Heidelberg. Available online at http://lib.myilibrary.com/detail.asp?id=265599.

Dubbel, Heinrich; Feldhusen, Jörg; Grote, Karl-Heinrich (2014): Dubbel. Taschenbuch für den Maschinenbau. Messtechnik. 24th ed. Berlin: Springer.

EURAMET/EMRP (2015): Traceable measurement of drivetrain components for renewable energy systems. Publishable JRP Summary Report for ENG56 DriveTrain, checked on 11/11/2015.

JCGM 100:2008, September 2008: Evaluation of measurement data - Guide to the expression of uncertainty in measurement.

Galyer, John Frederick Wise; Shotbolt, Charles Reginald (1990): Metrology for engineers. 5. (rev.) ed. London: Cassell.

DIN EN ISO 16610-21, 06.2013: Geometrische Produktspezifikation (GPS) - Filterung - Teil 21: Lineare Profilfilter: Gauß-Filter, checked on 3/1/2016.

Grabe, Michael (2011): Grundriss der Generalisierten Gauß'schen Fehlerrechnung. s.l.: Springer Berlin Heidelberg. Available online at http://lib.myilibrary.com/detail.asp?id=336684.

Hernla, Michael (2000): Application of Filter in the Evaluation of Measured Surface Profiles. In *Technisches Messen* (67), pp. 128-125.

International Energy Agency (IEA) (2015a): Recent energy trends in OECD. Excerpt from: Energy Balances of OECD countries 2015. Available online at http://www.iea.org/publications/freepublications/publication/EnergyBalancesofOECDcountries2015editionexcerpt.pdf, checked on 11/12/2015.

International Energy Agency (IEA) (2015b): World Energy Outlook 2015 Factsheets. Available online at http://www.worldenergyoutlook.org/media/weowebsite/2015/WEO2015_Factsheets.pdf, checked on 11/12/2015.

Juhanko, Jari (2011): Dynamic geometry of a rotating paper machine roll. Dissertation. Aalto University, Espoo, Finland. Department of Engineering Design and Production, checked on 8/24/2015.

Micro-Epsilon Messtechnik GmbH & Co. KG (Micro-Epsilon) (2015): confocalDT product catalog. Available online at http://www.micro-epsilon.de/download/products/cat--confocalDT--en.pdf, checked on 1/14/2016.

Mitutoyo Corp. (Mitutoyo) (2013): CRYSTA-Apex S Series. Bulletin No. 2097. Available online at http://www.mitutoyo.com/wp-content/uploads/2013/01/2097_CRYSTA_ApexS.pdf, checked on 11/19/2015.

Mitutoyo Corp. (Mitutoyo) (2014a): Legex 9106. Available online at http://www.mitutoyo.com.br/site/download/02folhetos/01%20Coordenadas/E16017.pdf, checked on 3/2/2016.

Mitutoyo Corp. (Mitutoyo) (2014b): ROUNDTEST RA-120/120P. Bulletin No. 2138. Available online at http://ecatalog.mitutoyo.com/cmimages/003/316/2138_RA-120-120P.pdf, checked on 11/19/2015.

Muralikrishnan, Bala; Raja, Jay (2009): Computational Surface and Roundness Metrology. London: Springer-Verlag. Available online at http://dx.doi.org/10.1007/978-1-84800-297-5.

Placko, Dominique (2006): Metrology in industry. The key for quality. London, Newport Beach, Calif.: ISTE USA. Available online at http://www.loc.gov/catdir/enhancements/fy0664/2006003530-d.html.

Rahman, Abdul Ghaffar Abdul; Chao, Ong Zhi; Ismail, Zubaidah (2011): Effectiveness of Impact-Synchronous Time Averaging in determination of dynamic characteristics of a rotor dynamic system. In *Measurement* 44 (1), pp. 34–45. DOI: 10.1016/j.measurement.2010.09.005.

Roberts, Donna (2012): Investigative Circle Activity Using Three Points. Oswego City School District Regents Exam Prep Center. Oswego. Available online at http://www.regentsprep.org/regents/math/geometry/gcg6/RCir.htm, checked on 1/12/2016.

Schaeffler Technologies AG & Co. KG (Schaeffler) (2016): Spherical roller bearing 23134 datasheet. Available online at http://medias.schaeffler.com/medias/de!hp.ec.br.pr/231.-E1A-K%20%2B%20AH*23134-E1A-K-M%20%2B%20AH, checked on 1/13/2016.

DIN ISO 1132-1, 09.2001: Wälzlager - Toleranzen - Teil 1: Begriffe.

DIN 620-1, 06.1982: Wälzlager; Meßverfahren für Maß- und Lauftoleranzen, checked on 9/1/2015.

Appendix

$$
\begin{aligned}
d = & \sqrt{\left(b1x + \frac{\frac{(b1x+b2x)(b2y-b3y)}{b2x-b3x} - \frac{(b2x+b3x)(b1y-b2y)}{b1x-b2x} + \frac{(b1y-b2y)(b1y-b3y)(b2y-b3y)}{(b1x-b2x)(b2x-b3x)}}{\frac{2\,b1y-2\,b2y}{b1x-b2x} - \frac{2\,b2y-2\,b3y}{b2x-b3x}}\right)^2} \\
& + \left(\frac{b2y}{2} - b1y + \frac{b3y}{2} + \frac{(b2x-b3x)\left(\frac{b2x}{2} + \frac{b3x}{2} + \frac{\frac{(b1x+b2x)(b2y-b3y)}{b2x-b3x} - \frac{(b2x+b3x)(b1y-b2y)}{b1x-b2x} + \frac{(b1y-b2y)(b1y-b3y)(b2y-b3y)}{(b1x-b2x)(b2x-b3x)}}{\frac{2\,b1y-2\,b2y}{b1x-b2x} - \frac{2\,b2y-2\,b3y}{b2x-b3x}}\right)}{b2y-b3y}\right)^2 \\
& - \left(\frac{\frac{(b1x+b2x)(b2y-b3y)}{b2x-b3x} - \frac{(b2x+b3x)(b1y-b2y)}{b1x-b2x} + \frac{(b1y-b2y)(b1y-b3y)(b2y-b3y)}{(b1x-b2x)(b2x-b3x)}}{\frac{2\,b1y-2\,b2y}{b1x-b2x} - \frac{2\,b2y-2\,b3y}{b2x-b3x}} + (a1x-a2x)\left(\frac{\frac{b2y}{2} + \frac{b3y}{2} + \frac{(b2x-b3x)\left(\frac{b2x}{2} + \frac{b3x}{2} + \frac{\frac{(b1x+b2x)(b2y-b3y)}{b2x-b3x} - \frac{(b2x+b3x)(b1y-b2y)}{b1x-b2x} + \frac{(b1y-b2y)(b1y-b3y)(b2y-b3y)}{(b1x-b2x)(b2x-b3x)}}{\frac{2\,b1y-2\,b2y}{b1x-b2x} - \frac{2\,b2y-2\,b3y}{b2x-b3x}}\right)}{b2y-b3y}}{a1y-a2y}\right)(a1y-a2y)\right) \\
& \Bigg/ \sqrt{\frac{(a1y-a2y)^2}{(a1x-a2x)^2} + 1}\,(a1x-a2x)
\end{aligned}
$$

Figure 6.1: Bearing element thickness based on 5 point measurement